KfK 5309
März 1994

Corrosion Studies on Selected Metallic Materials for Application in Nuclear Waste Disposal Containers

E. Smailos, B. Fiehn, J. A. Gago, I. Azkarate
Institut für Nukleare Entsorgungstechnik

Kernforschungszentrum Karlsruhe

Kernforschungszentrum Karlsruhe
Institut für Nukleare Entsorgungstechnik

KfK 5309

CORROSION STUDIES ON SELECTED METALLIC MATERIALS FOR APPLICATION IN NUCLEAR WASTE DISPOSAL CONTAINERS

E. Smailos, B. Fiehn, J.A. Gago *, I. Azkarate **

*ENRESA, Spain
**INASMET, Spain

Annual report 1993 prepared within the framework of the 1991-1994 programme of the European Atomic Energy Community: "Management and storage of radioactive waste". Task 3: Characterization and qualification of waste forms, packages and their environment. EC-Research Contract No. FI2W-CT90-0030.

Kernforschungszentrum Karlsruhe GmbH, Karlsruhe

Kernforschungszentrum Karlsruhe GmbH
Postfach 3640, 76021 Karlsruhe

ISSN 0303-4003

Summary

In previous corrosion studies, carbon steels and the alloy Ti 99.8-Pd were identified as promising materials for heat-generating nuclear waste containers acting as a radionuclide barrier in a rock-salt repository. To characterize the long-term corrosion behaviour of these materials in more detail, a research programme including laboratory-scale and in-situ corrosion studies has been undertaken jointly by KfK and ENRESA/INASMET. Besides carbon steels and Ti 99.8-Pd, also Hastelloy C4 and some Fe-base materials are being examined in order to complete the results available to date.

In the period under review, gamma irradiation corrosion studies of up to about 6 months at 10 Gy/h and stress corrosion cracking studies at slow strain rates (10^{-4}-10^{-7} s^{-1}) were performed on three preselected carbon steels in disposal relevant brines (NaCl-rich, $MgCl_2$-rich) at 90°C and 150°C. Moreover, results were obtained from long-term in-situ corrosion studies (maximum test duration 9 years) conducted on carbon steel, Ti 99.8-Pd, Hastelloy C4, Ni-resist D4, and Si-cast iron in boreholes in the Asse salt mine.

In the in-situ experiments, tubes of the above-mentioned materials provided with selected container manufacturing characteristics were tested in addition to metal sheets. Two types of tubes were examined: Tubes with the container sealing technique simulated by electron beam (EB) and tungsten inert gas (TIG) welding, respectively, and carbon steel tubes in which a corrosion protection with either Ti 99.8-Pd or Hastelloy C4 was simulated by explosion plating. The in-situ tested specimens were exposed to rock salt and rock salt plus brines, respectively, at temperatures of 32°C-200°C.

The results obtained from the 6-month irradiation corrosion studies at 150°C and 10 Gy/h indicate that the unalloyed fine-grained steel TStE 355 is subjected to general corrosion in the brines. In the irradiated NaCl-brine, the corrosion rate of the steel (15 µm/a) is very close to that in the unirradiated brine (19 µm/a). In the $MgCl_2$-rich brines, the corrosion rates in the presence of radiation (124-220 µm/a) are higher by a factor of about 1.3-1.8 than those without irradiation. However, such corrosion rates imply corrosion allowances technically acceptable for thick-walled containers.

The in-situ corrosion studies show that all material specimens (metal sheets and tubes) are resistant to pitting corrosion in rock salt and rock salt plus brine and that the general corrosion rates are negligibly small. Only in rock salt plus $MgCl_2$-rich brine, the non-corrosion protected carbon steel tube exhibited significant non-uniform general corrosion of about 90 µm/a.

In the slow strain rate tests at 10^{-4}-10^{-7} s^{-1} and 90°C, a loss of ductility occurred for the steels in the MCl_2-rich brine compared to argon, which is probably due to hydrogen embrittlement. However, this effect is not significant and no indication of stress corrosion cracking was found for the hot-rolled steels TStE 355 and TStE 460. On the contrary, the forged steel 15 MnNi 6.3 is susceptible to stress corrosion cracking at a rate of 10^{-7} s^{-1}. Further corrosion studies are in progress.

Korrosionsuntersuchungen an ausgewählten Verpackungsmaterialien für die Endlagerung von wärmeerzeugenden radioaktiven Abfällen in Steinsalzformationen

Zusammenfassung

Bisherige Korrosionsuntersuchungen ergaben, daß Kohlenstoffstähle und die Legierung Ti 99.8-Pd aussichtsreiche Materialien für langzeitbeständige Behälter zur Endlagerung von wärmeerzeugenden Abfällen in Steinsalzformationen sind. Zur detaillierten Charakterisierung des Korrosionsverhaltens dieser Werkstoffe werden von KfK und ENRESA/INASMET in einem gemeinsamen Forschungsprogramm weitergehende Untersuchungen durchgeführt. Neben Stählen und Ti 99.8-Pd werden zur Vervollständigung der bisher vorliegenden Ergebnisse auch Hastelloy C4 und einige Eisenbasiswerkstoffe untersucht.

Im Berichtszeitraum wurden Langzeit-Korrosionsuntersuchungen (Immersionsexperimente) unter Gamma-Bestrahlung (10 Gy/h, 150°C) und Spannungsrißkorrosionsexperimente bei langsamen Dehnungsraten (10^{-4}-10^{-7} s^{-1}, 90°C) an drei vorausgewählten Stählen in Salzlösungen durchgeführt. Darüber hinaus wurden Ergebnisse aus Langzeit-in situ-Korrosionsexperimenten (maximale Versuchsdauer 9 Jahre) an Stahlguß, Ti 99,8-Pd, Hastelloy C4 und den Eisenbasislegierungen Ni-Resist D4 und Si-Guß gewonnen.

In den in situ-Experimenten, die in Bohrlöchern im Salzbergwerk Asse durchgeführt wurden, wurden neben Metallblechen aus den oben genannten Werkstoffen, Rohrabschnitte versehen mit ausgewählten Herstellungsmerkmalen für Behälter geprüft. Es wurden zwei Arten von Rohrabschnitten untersucht: Rohrabschnitte mit simulierter Behälterverschlußtechnik durch Elektronenstrahlschweißen oder Wolfram-Inertgas-Schweißen und Stahlguß-Rohrabschnitte, in denen ein Korrosionsschutz aus Ti 99,8-Pd bzw. Hastelloy C4 durch Sprengplattieren simuliert wurde. Bei den in situ-Experimenten wurden die Proben dem korrosiven Angriff von Steinsalz (0,1 Gew.% H_2O) bzw. Steinsalz plus Salzlösung bei Temperaturen zwischen 32°C und 200°C ausgesetzt.

In Gegenwart eines Gamma-Strahlenfeldes von 10 Gy/h ist der untersuchte unlegierte Feinkornbaustahl beständig gegenüber Lochkorrosion in allen Lösungen und seine Korrosionsrate in NaCl-reicher Lösung (15 µm/a) entspricht weitestgehend dem Wert in der unbestrahlten Lösung (19 µm/a). In bestrahlten $MgCl_2$-reichen Lösungen sind die Korrosionsraten des Stahls (124-220 µm/a) etwa um den Faktor 1,3-1,8 höher als ohne Bestrahlung. Solche Korrosionsraten führen zu technisch akzeptablen Korrosionszuschlägen für dickwandige Endlagerbehälter.

Die in situ-Korrosionsexperimente zeigen, daß alle untersuchten Werkstoffe (Stahlguß, Ti 99,8-Pd, Hastelloy C4, Ni-Resist D4 und Si-Guß) beständig gegenüber Lochkorrosion in Steinsalz und in Steinsalz plus Salzlösung sind und daß die Flächenkorrosion vernachläßigbar klein ist. Nur in Steinsalz plus $MgCl_2$-reiche Lösung tritt bei Stahlguß eine starke Flächenkorrosion von 90 µm/a auf.

In den Korrosionsuntersuchungen in einer $MgCl_2$-reichen Lösung bei 90°C und Dehnungsraten von 10^{-4} - 10^{-7} s^{-1} nimmt die Duktilität der Stähle gegenüber Argon deutlich ab, was möglicherweise auf eine H_2-Versprödung zurückzuführen ist. Allerdings ist dieser Effekt nicht signifikant und es waren keine Anzeichen für eine Spannungsrißkorrosion bei den warmgewalzten Stählen TStE 355 undTStE 460 festzustellen. Der Schmiedestahl 15 MnNi 6.3 hingegen zeigt in der Lösung bei einer Dehnungsrate von 10^{-7} s^{-1} eine Anfälligkeit gegenüber Spannungsrißkorrosion. Weitere Korrosionsuntersuchungen sind im Gange.

Table of Contents

1. INTRODUCTION AND OBJECTIVES

According to the German concept, the heat-generating nuclear waste such as vitrified high-level waste and spent fuel will be disposed of in repositories located in deep rock-salt formations. The isolation of the radionuclides from the biosphere shall be ensured by a combination of geological and engineered barriers. One element of this multi-barrier concept is the waste packaging. Consequently, studies have been undertaken by KfK within the framework of the European Community research programme to qualify materials for long-lived packagings that could act as a radionuclide barrier during the elevated-temperature phase in the disposal area, which lasts a few hundred years. The main requirement made on the packaging materials is their corrosion resistance in rock salt and salt brines. Salt brines in the disposal area may originate from the thermal migration of brine inclusions in the rock salt and have to be considered in accident scenarios, e.g. brine inflow through an anhydride layer.

In previous corrosion studies on a wide range of materials in salt brines [e.g. 1,2], two materials were identified as the most promising for the manufacturing of long-lived containers surrounding the Cr-Ni steel waste canisters. These are: The passively corroding alloy Ti 99.8-Pd for a corrosion resistant concept and the actively corroding carbon steels for a corrosion allowance concept. To characterize the corrosion behaviour of these materials in more detail, a 1991-1994 EC research programme is being performed jointly by KfK and ENRESA/INASMET (Spain).

The research programme consists of two parts. The KfK part is aimed at studying the influence of important parameters on the long-term corrosion behaviour of four preselected carbon steels (two unalloyed, two low-alloyed) and Ti 99.8-Pd in disposal relevant salt brines. These parameters are: Temperature, gamma radiation and selected characteristics of packaging manufacturing. Both, laboratory-scale immersion experiments and in-situ corrosion studies in the Asse salt mine are being carried out.

The second part of the corrosion studies concerns the investigation of resistance of the carbon steels to stress corrosion cracking in a disposal relevant salt brine at variable strain rates and temperatures by ENRESA/INASMET. For this purpose, the slow strain rate technique (SSRT) is being applied. These studies serve to complete

the results available so far on statically loaded U-bent specimens. The entire research programme is coordinated by KfK.

In the present paper, the progress achieved in the research programme within the period of January to December 1993 shall be described.

2. GAMMA IRRADIATION-CORROSION STUDIES ON THE UNALLOYED FINE-GRAINED STEEL (KfK)

An essential aspect of the corrosion studies on container materials is the investigation of the influence exerted by the radiation of the waste on their corrosion behaviour in disposal relevant brines. Of the various types of radiation, only gamma radiation is present at the surface of the container. The dose rate depends on the design of the container and the nature of the waste inside. For HLW carbon steel containers acting as a radionuclide barrier in a rock-salt repository, a wall thickness of about 100 mm is needed for mechanical support against the rock pressure of 36±5 MPa [3] at 1000 m disposal depth. In this case, the expected gamma dose rate on the surface of the container will be about 10 Gy/h.

Corrosion studies under gamma irradiation are important because the interaction of gamma radiation with salt brines produces reduced/oxidizing reactive particles and stable products such as e^-_{aq}, H_2, Cl_2^-, H_2O_2, ClO_3^-, etc. [4] which may change the rate and mechanism of corrosion. Consequently, the corrosion behaviour of a preselected unalloyed steel (fine-grained steel) is being examined up to 18 months in salt brines in the presence of a gamma radiation field at high temperature. In the following, the results obtained in the period under review are reported about.

2.1 Steel investigated and test conditions

The preselected unalloyed fine-grained steel TStE 355 was examined in the hot-rolled and normalized condition. The metal sheet used for the preparation of the corrosion specimens had the following composition in wt.%:

C: 0.17; Si: 0.4; Mn: 1.49; P+S: < 0.1; bal.: Fe.

For the corrosion studies, plane specimens with dimensions of 40x20x4 mm were used. Prior to specimen fabrication, the metal sheet was freed from the adhering

oxide layer by milling. After this mechanical treatment, the specimens were cut and cleaned with alcohol in an ultrasonic bath.

To have severe test conditions, the steel was investigated simulating an accident with an intrusion of large amounts of brine into the disposal area. To examine the influence of the brine composition on the corrosion behaviour of the steel, three disposal relevant salt brines differing qualitatively and quantitatively were used as the corrosion media. Two of them, brine 1 (Q-brine) and brine 2 are highly concentrated in $MgCl_2$, the third one (brine 3) has a high concentration of NaCl. The compositions and the measured pH and O_2-values of the test brines are given in Table I. The pH values given are relative data and were measured using a glass electrode. Application of the correction formula proposed by Bates et al. [5] gives pH values at 25°C which are higher than the measured values by 1.8-2.2 units for the brines 1 and 2, and by 0.4 units for the brine 3. The O_2-values of the brines were determined by a polarographic method using an O_2-sensor; the saturation values (1.0-1.4mg O_2/l) obtained by the Winkler method were used as the reference values.

The steel was examined for general and local corrosion in the brines at a realistic gamma dose rate of 10 Gy/h for the thick-walled container discussed. For comparison, also corrosion tests without radiation were carried out. A test temperature of 150°C was selected which roughly corresponds to the maximum temperature on the surface of the container according to the German concept. The experiments lasted up to 166 days. Experiments of up to 18 months are in progress.

2.2 Experimental set-up

The corrosion experiments under gamma irradiation were performed in the spent fuel storage pool of KFA Jülich. The radiation source were spent fuel elements with a gamma energy spectrum similar to that of 10-years-old vitrified HLWC. The experimental set-up is shown schematically in Fig. 1. For the experiments, autoclaves made of the corrosion resistant alloy Ti 99.8-Pd with insert vessels of Duran glass were used. The autoclaves were placed in a circular configuration into heated cylindrical stainless steel containers (irradiation containers). Each glass insert contained 120 ml of brine and three specimens of 60 cm^2 total surface, which were totally immersed into the brine. This gave a brine volume to specimen surface ratio of 2 ml/cm^2. The specimens were suspended from a frame

made of a glass-fibrereinforced plastic. For irradiation, the stainless steel containers were positioned at the bottom of the 6 m deep water-filled spent fuel element storage pool. The specimens and brines were heated to the test temperature of 150°C using heaters.

For the experiments in unirradiated brines (V/S=2 ml/cm^2) at 150°C, stainless steel pressure vessels provided with corrosion resistant insert vessels made of PTFE were used to avoid evaporation of the brines (boiling point: about 115°C). These vessels were filled which the brines, into which the specimens were immersed. After the pressure vessels had been closed, they were stored in heating chambers at 150°C. The experiments were performed at equilibrium pressure of 0.4 MPa. To determine the corrosion kinetics, the specimens were examined at various immersion times.

2.3. Post-test examination of the specimens

When the specified test duration had been reached, the specimens were removed from the brines and treated according to the ASTM guidelines. For this purpose, the specimens were freed from the adhering salts and corrosion products by cleaning in distilled H_2O at 60°C and pickling in the Clark solution (37% $HCl+Sb_2O_3+SnCl_2$) with subsequent cleaning in distilled H_2O and alcohol. After drying, the specimens were examined for general and local corrosion. General corrosion was calculated from the gravimetrically determined integral weight losses and the material density. The examination for local corrosion was made by microscopic evaluation, measurements of pit depth, surface profilometry and metallography.

2.4 Results

The integral weight losses and the corrosion rates of the steel after an 166-day-exposure to irradiated and unirradiated brines at 150°C are compiled in Table II. For comparison, the results of previous studies [6] lasting 100 days are given as well. All values are the average values of 3-4 specimens. In both cases with and without gamma radiation, the integral corrosion rates of the steel in the $MgCl_2$-rich brines 1 and 2 are significantly higher than in the NaCl-rich brine 3. The highest corrosion rate occurs in the $MgCl_2$-richest brine 2, the lowest in the NaCl-rich brine 3. The higher corrosivity of the $MgCl_2$-rich brines compared to the NaCl-rich brine is attributed to their higher HCl concentration. This can be explained by

the higher Cl^- concentration and the hydrolysis of Mg^{2+}. The acceleration of the steel corrosion in brines containing high amounts of $MgCl_2$ is in agreement with the results reported by Westerman et al. [7].

The imposition of a 10 Gy/h radiation field on the 150°C brine environment increases the average integral corrosion rates of the steel specimens in the brines 1 and 2 from about 60 µm/a to 124 µm/a, and from 170 µm/a to 221 µm/a, respectively. In brine 3, the corrosion rate in the 10 Gy/h irradiated environment (14.6 µm/a) is very close to the value attained in the unirradiated system (19.2 µm/a).

Surface profiles and metallographic examinations of corroded specimens have shown that the steel is resistant to pitting corrosion in both irradiated and unirradiated brines. In all brines, a non-uniform general corrosion was observed. However, the measured maximum penetration depth of this uneven corrosion corresponds to the values of the average thickness reduction. Figure 2 shows optical micrographs of steel specimens after 166 days of exposure to the test brines at 150°C and 10 Gy/h.

3. IN-SITU CORROSION STUDIES ON SELECTED CONTAINER MATERIALS (KfK)

On the basis of the corrosion results obtained so far and considering mechanical aspects, a thick-walled carbon steel container with or without a corrosion protection made of Ti 99.8-Pd was identified for the packaging of the wastes [8,9]. As an alternative to Ti 99.8-Pd, the suitability of Hastelloy C4 as a corrosion protection material is being examined. Both, in-depth laboratory-scale and in-situ corrosion studies are being performed.

An important aspect of the in-situ studies is the investigation of the influence of selected container manufacturing characteristics (e.g. sealing technique, application mode of the corrosion protecting layer on the steel) on the corrosion of the materials. Therefore, two types of cast steel tubes are being examined besides metal sheets, under simulated disposal conditions in heated boreholes in the Asse salt mine:

- Non-corrosion protected cast steel tubes with the container sealing technique being simulated by electron beam (EB) welding.

- Corrosion protected cast steel tubes with the corrosion protection of either Ti 99.8-Pd or Hastelloy C4 being simulated by explosion plating and electron beam welding.

In addition to the cast steel tubes, some investigations are being performed on electron beam and tungsten inert gas (TIG) welded tubes made of Ni-resist D4 (an Fe-base material) and Ti 99.8-Pd in order to complete the results available to date.

In-situ corrosion results obtained for metal sheets and tubes after 1.5-3 years of exposure to rock salt and rock salt plus brine have already been reported about [2,10,11]. In the period under review, the long-term in-situ corrosion experiments lasting up to about 9 years for metal sheets and 6 years for tubes, respectively, were completed and the specimens were examined for corrosion attacks.

3.1 Testing of metal sheets

Metal sheets of Ti 99.8-Pd, Hastelloy C4 and the two Fe-base materials Ni-resist D4 and Si-cast iron were investigated for 9 years in loose rock salt at the rock temperature of 32°C. For this, material specimens were stored in small boreholes (50 mm diameter, 200 mm length) at the 775 m level of the Asse salt mine and covered with salt grit. The composition of the materials investigated is evident from Table III. The rock salt had the following average composition (wt.%).

Na^+: 38.3; K^+: 0.33; Ca^{2+}: 0.17; Mg^{2+}: 0.16;
Cl^- : 58.02; SO_4^{2-}: 2.47; H_2O: 0.1.

For Ni-resist and Si-cast iron, only the parent materials (as received) were studied. For the most promising HLW container materials Ti 99.8-Pd and Hastelloy C4, the influence of welding on the corrosion behaviour was studied with respect to container closing by welding in a later application. For this purpose, specimens were examined with a TIG (Tungsten Inert Gas) weld beam applied.

All material specimens were examined for their resistance to general corrosion (weight change) and local corrosion by gravimetry, surface profilometry and metallography. Plane specimens with the following dimensions were used: Ti 99.8-Pd, Hastelloy C4 and Si-cast iron: 40 mm x 20 mm x 4 mm; Ni-resist D4: 50 mm x 10 mm x 10 mm.

The integral weight losses of the specimens after 9 years of testing at 32°C and the integral corrosion rates calculated from them are presented in Table IV. The values are average values of three specimens. No measurable corrosion attack was observed on Ti 99.8-Pd. Moreover, the corrosion rates were very small (0.17-1.14 µm/a) for the materials Hastelloy C4, Ni-resist D4 and Si-cast iron . The surface profiles and the metallographic examinations of the specimens in the as-received and welded conditions did not provide any indications of local corrosion.

3.2 Testing of welded tubes

3.2.1 Test field and details of the specimens

The configuration and dimensions of the underground test field at the 775 m level in the Asse salt mine are shown in Fig. 3. The composition of the rock salt taken from the test field boreholes is given in section 3.1.

In the reporting time, the following eight tubes were investigated under simulated disposal conditions (see section 3.2.2):

- Five electron-beam (EB) welded cast steel tubes (GS 16 Mn5). Two do not have any corrosion protection, two are provided with a corrosion protection layer of Ti 99.8-Pd, and one with Hastelloy C4 applied by explosion plating and EB-welding.

- One tungsten inert gas (TIG) welded tube made of Ti 99.8-Pd.

- Two electron-beam welded tubes made of the Fe-base material Ni-resist D4.

The tube materials used had the following compositions in wt.%:

Cast steel: 0.16 C; 0.66 Si; 1.51 Mn; 0.02 P+S; bal. Fe.

Ti 99.8-Pd: 0.2 Pd; 0.03 Fe; bal. Ti.

Hastelloy C4: 15.5 Cr; 15.3 Mo; 0.8 Fe; bal. Ni.

Ni-resist D4: 30.9 Ni; 5.5 Cr; 2.6 C; 4.25 Si; 0.5 Mn; bal. Fe.

The specimens of cast steel and Ni-resist D4 consisted of nine tube sections (50 mm length, 45 mm outside diameter, 20 mm inside diameter each) and a bottom part which was joined by EB-welding to simulate a container sealing technique. Thus, tubes of 500 mm total length were obtained. Figure 4 shows a cast steel specimen by way of example. The Ti 99.8-Pd specimen was a tube (L=500 mm, D=25.4 mm) with a longitudinal weld and a TIG-welded bottom. More detailed information on the manufacturing of the specimens can be found elsewhere [12].

3.2.2 Test conditions and experimental set-up

The tubes were tested under the following conditions:

- Two cast steel tubes with and without corrosion protection made of Ti 99.8-Pd, and two Ni-resist D4 tubes were tested for 5.3 years in the Asse rock salt (H_2O content: 0.1 wt.%) at HLW design temperature ($T_{max.}$=200°C). Thus, the normal operating conditions of a repository were simulated.

- Three carbon steel tubes with and without corrosion protection of Ti 99.8-Pd or Hastelloy C4, and one TIG-welded Ti 99.8-Pd tube were tested under the conditions of a hypothetical inflow of brine into the HLW boreholes during the initial disposal phase. This means while the annular gap between the container and the borehole wall was still open. The carbon steel tubes were tested for 6.3 years both in an $MgCl_2$-rich brine (Q-brine) and in saturated NaCl-brine at rock temperature of 32°C. The Ti 99.8-Pd tube was examined for 2.8 years only in NaCl-brine at $T_{max.}$ = 200°C.

Each tube was placed into a heated vertical borehole of 2 m depth at the 775 m level of the Asse salt mine (see Fig. 5). At the beginning of the experiments, a 1 mm wide annular gap existed between the tubes and the borehole wall. In the experiments with brine as the corrosion medium, the annular gap was filled with 100 ml Q-brine (26.8 wt.% $MgCl_2$; 4.7 wt.% KCl; 1.4 wt.% $MgSO_4$; 1.4 wt.% NaCl; 65.7 wt.% H_2O) or NaCl-brine (26.9 wt.% NaCl; 73.1 wt.% H_2O).

The temperature of 200°C was set at the borehole wall using a heater. The radial temperature distribution between two boreholes and the vertical temperature profile developed during the experiments at the contact surface between the tube and the borehole wall are shown in Figs. 6 and 7. The maximum tem-

perature of 200°C occurred in the centre of the heated zone, the minimum temperature of 90°C was measured in the upper tube zone. The temperature in the centre between two boreholes nearly corresponded to the rock salt temperature of about 32°C at the 775 m level. The temperature was measured using NiCr-Ni thermocouples. In order to avoid invalidation of the corrosion results due to the corrosion induced by the contact of the thermocouples and tube surface, the temperature measurements were performed in reference boreholes of identical experimental set-up. In the experiments with the presence of brine and T = 200°C, the pressure in the annular gap of the real test boreholes was measured continuously with a manometer, which was introduced into the brine inlet tube. The maximum pressure measured was 0.28 MPa which corresponds to a salt brine boiling point of 140°C. This means that the water contained in the brine evaporates at points of elevated temperature and recondenses at the upper cooler end of the tube (90°C).

Like the temperatures, the stresses prevailing on the tube surface were measured in reference boreholes using strain gauges. The measurements have shown that the first contact of the borehole wall with the tube due to rock pressure occurred after about six months. On the basis of the results obtained in an identical preliminary test [12], complete closure of the 1 mm wide annular gap would have taken place after approximately twelve months.

3.2.3 Post-test examination of the specimens

When the specified test duration was reached, the tubes were retrieved by overcoring. The salt drilling cores obtained (1 m length, 120 mm outside diameter) were cut into two half shells and visual inspection of the tubes and the drilling cores was made, if required. The tubes were freed from the adhering salts and corrosion products, by mechanical treatment, cleaning in H_2O at 60°C and pickling in diluted HCl. Then the tubes were cleaned in distilled H_2O and alcohol. After drying, the tubes were subjected to post-test examination for corrosion attack by means of surface profilometry and metallography.

3.2.4 Results

Visual inspection of the drilling cores indicated that the 1 mm annular gap between the tubes and the borehole wall existing at the beginning of the experiments had completely closed. In the experiments with brine at 90°C-200°C,

dissolved salt was clearly visible below the ceramic insulation in the cooler upper part of the tube (T = 90°C). This was attributed to the condensation of water vapour. The microscopic evaluation of microsections taken from the drilling cores revealed that the heat and the brines added caused changes in the surrounding rock salt. Zones of crystallized brine, corroded grain boundaries of rock salt, etc. were observed.

The surface profiles and the metallographic examinations of specimens show that corrosion of a non-corrosion protected cast steel tube in rock salt containing a small amount of water (0.1 wt.%) is negligibly small. Neither on the parent material nor on the EB-welds were any signs of pitting corrosion or stress corrosion cracking found. After 5.3 years of testing at 90°C-200°C, a general corrosion of about 10 µm only was observed over the initial roughness of the tube surface (30-35 µm). Figure 8 shows an optical micrograph of a cast steel tube section after exposure to rock salt.

In rock salt plus $MgCl_2$-rich Q-brine (6.3 years at 32°C), the non-corrosion protected cast steel tube also was resistant to pitting corrosion and stress corrosion cracking. However, the tube suffered from significant general corrosion with voluminous corrosion products present. This corrosion attack was non-uniformly distributed on the tube surface (see optical micrograph Fig. 9) such that the individual tube areas exhibited significant differences in the penetration depth. This indicates that certain tube parts were exposed to a larger brine volume than others. This is attributed to the irregular distribution of the brine in the annular gap as a consequence of irregularities in the shape of the borehole and the positioning of the tube.

Figure 10 shows the maximum penetration depth of corrosion in various sections of the cast steel tubes exposed to rock salt (very small corrosion) and to rock salt plus brine (extensive corrosion). It is evident that in rock salt plus brine the greatest corrosion attack of 570 µm occurred at the lower part of the tube, while the smallest of 180 µm existed at the top of the tube. These values determined after 6.3 years of test duration at 32°C correspond to average corrosion rates of about 30 µm/a (top of the tube) and 90 µm/a (bottom), respectively, and are smaller than those obtained in previous studies [10] at 90°C-200°C. A possible explanation for the smaller corrosion of the upper tube part is the lowering of the brine level in the borehole during the test period due to water consumption

by the corrosion reaction with Fe. This means that the upper tube part was not exposed to brine during the entire test period.

The Ni-resist tubes tested in rock salt (5.3 years at 90°C-200°C) and the Ti 99.8-Pd tube examined in rock salt plus NaCl-brine (2.8 years at 90°C-200°C) were found to be resistant to general and local corrosion as well as and to stress corrosion cracking. For Ni-resist D4, very little general corrosion of about 5-10 µm was detected after about 5 years of testing. In case of Ti 99.8-Pd, corrosion attacks were found neither on the parent material nor on the TIG-welded bottom of the tube. Figures 11 and 12 show optical micrographs of Ni-resist and Ti 99.8-Pd tubes after in-situ testing.

The examination of the cast steel tubes provided with a corrosion protection of Ti 99.8-Pd and Hastelloy C4, respectively, has not shown any changes on the surface of the plating materials by corrosion attacks in rock salt or rock salt plus brine. Neither on the mechanically finished surface nor on the hot-rolled and electron beam welded sheet metal surface were any signs of corrosion observed. Even the crack produced by a steel needle in order to simulate severe conditions due to handling of the containers did not stimulate a corrosion attack. Figures 13 and 14 show optical micrographs of the plating materials Ti 99.8-Pd and Hastelloy C4 after testing in rock salt and rock salt plus brine.

4. STRESS CORROSION CRACKING TESTING OF CARBON STEELS (ENRESA/INASMET)

The resistance of three preselected carbon steels to stress corrosion cracking is being examined in the $MgCl_2$-rich Q-brine (26.8 wt.% $MgCl_2$; 4.7 wt.% KCl; 1.4 wt.% $MgSO_4$; 1.4 wt.% NaCl; 65.7 wt.% H_2O) by means of the slow strain rate technique (SSRT). The steels to be investigated are the low-alloyed steels TSt E 460 and 15MnNi 6.3 and the unalloyed fine-grained steel TSt E 355. The steels have the following compositions in wt.%:

TSt E 460:	0.18 C; 0.34 Si; 1.5 Mn; 0.51 Ni; 0.15 V; bal. Fe
15MnNi 6.3:	0.17 C; 0.22 Si; 1.59 Mn; 0.79 Ni; bal. Fe
TSt E 355:	0.16 C; 0.41 Si; 1.5 Mn; bal. Fe.

The experiments are performed in Hastelloy C-276 autoclaves at strain rates of 10^{-4}-$10^{-7}s^{-1}$, temperatures of 25°C, 90°C and 170°C, and an argon pressure of 13MPa. In order to be able to interpret the results obtained in the brine, additional comparative investigations are carried out in argon as the inert medium. Besides specimens made of the parent materials, also MAG (Metal Active Gas) welded specimens simulating a possible container closure technique are being tested.

Experimental results obtained for the three steels at 170°C have already been reported in previous work [6,11]. In the period under review, stress corrosion cracking studies were conducted on unwelded and MAG welded steel specimens at 90°C.

4.1. Materials and experimental

The parent materials of TSt E 355 and TSt E 460 were hot-rolled and annealed plates, while for 15MnNi 6.3 forged and annealed disks were used. For the steels TSt E 355 and TSt E 460, a ferritic microstructure with perlite bands typical of the rolling process was observed. A grain size value of 10 according to ASTM E- 112 was measured for both steels. For the forged steel 15 MnNi 6.3, a ferrite-perlite microstructure of a duplex grain size with an average value of 9 (according to ASTM E- 112) was observed. For the MAG-welding of the steels, filler materials (Griduct SV-8 for TSt E 355 and Thyssen Union K-5 for TSt E 460 and 15MnNi 6.3) were used. The mechanical properties of the parent materials are given in Table V.

For the slow strain rate tests, round specimens of 6 mm diameter were machined and finished with 1000 grade emery paper. The TSt E 355 and TSt E 460 specimens were machined in transverse direction to the rolling direction of the plates, those of 15MnNi 6.3 in the radial direction of the forged disks. The specimens were located in the Hastelloy C 276 autoclaves with one end being attached to a fixed frame and the other to the pull rod. Fittings made of ZrO_2 ensured the electrical insulation of the specimens. Then, the autoclave was filled either with Q-brine or argon, closed, pressurized and heated. Once the testing temperature and pressure were reached, the specimens were pulled until fracture at the selected actuator displacement speed.

Load, position, time and temperature data were continuously logged by the microprocessor that controls the testing machine. After each test, the elongation (E), reduction of area (R.A.), energy, yield strength (Y.S.), maximum load, and true stress at fracture were calculated. To evaluate the resistance of the steels to stress corrosion cracking, metallographic and scanning electron microscopic (SEM) examinations of the fracture specimen surfaces were performed in addition to the tensile experiments.

4.2 Results

The results of the slow strain rate tests obtained for the unwelded (parent materials) and MAG-welded steel specimens in argon and Q-brine at 90°C and variable strain rates (10^{-4}-10^{-7} s^{-1}) are given in Figs. 15 through 18. All values are the average of at least two experiments. The values of the yield strength and maximum load in Q-brine are very close to those in argon. However, a clear decrease of the elongation, reduction of area, energy and true stress at fracture occurs for all steels in Q-brine at 90°C in comparison to argon. This finding is in good agreement with own previous results at 170°C [6] and those reported by Westerman et al. [7]. Nevertheless, the loss of ductility of the steels at 90°C is lower than that at 170°C. The results obtained for the MAG-welded steel specimens show that the reduction of ductility in Q-brine compared to argon is very similar to that observed for the parent materials.

In the metallographic examinations of steel specimens tested in Q-brine, a non-uniform general corrosion due to repeated breaking of the corrosion surface layer was observed for all steels both in the unwelded and MAG-welded conditions (Figs. 19-20). Secondary cracks typical for stress corrosion cracking were not observed for the hot-rolled steels TStE 355 and TStE 460 under any of the test conditions. For this reason, the reduction of ductility of these steels in Q-brine compared to argon cannot be attributed to stress corrosion cracking. For the loss of ductility in this brine, another mechanism such as embrittlement may be responsible. Also in case of the forged steel 15MnNi 6.3, no signs of sensitivity to stress corrosion cracking were found in Q-brine at 90°C and strain rates up to 10^{-6} s^{-1}. However, at the slowest strain rate of 10^{-7} s^{-1}, extensive lateral secondary cracks indicating stress corrosion cracking were observed, besides a non-uniform corrosion (Fig. 21).

To quantify and compare the stability of the steels to stress corrosion cracking in Q-brine, the crack density on the lateral surface of the specimens, the maximum crack length and the crack length/width ratio parameters have been measured. The results obtained for specimens tested in the brine at 90°C and 170°C [6] are plotted in Figs. 22-24. The parameter crack length/width ratio (Fig. 24) gives an idea of the sharpness of the crack, and is the most interesting one to quantify the stress corrosion cracking resistance of a material. According to these data, the hot-rolled steel TStE 355 is the most and the forged steel 15MnNi 6.3 the least resistant material to stress corrosion cracking in the brine. Comparison of the maximum crack lengths brings about the same results.

The fracture surface features observed in the scanning electron microscopic (SEM) examinations show a change from a fully ductile manner when steel specimens are tested in argon to a brittle one when the specimens are tested in Q-brine (Figs. 25-27). The embrittlement of the steels in Q-brine at slow strain rates is probably due to the hydrogen produced during corrosion, as already discussed in previous work [6]. It appears that the hydrogen enters the steels in the atomic form, predominantly in zones of a high stress level and causes a loss of ductility. However, this is not serious because the residual reduction of area and elongation at fracture of the steels are still relatively high after testing in the brine environment.

5. CONCLUSIONS

The 6-month irradiation corrosion studies at 150°C indicate that a gamma dose rate of 10 Gy/h does not cause an increase in corrosion rate of the fine-grained steel TStE 355 over that found in the unirradiated brine environment. In irradiated $MgCl_2$-rich brines, the corrosion rate of the steel is higher by about a factor of 1.3-1.8 (depending on the brine composition) than in the non-irradiated brines. As in the experiments without irradiation, no pitting corrosion was observed for the steel in the presence of radiation.

The results of the in-situ studies show that corrosion of cast steel, Ni-resist D4, Ti 99.8-Pd and Hastelloy C4 in rock salt at temperatures of up to 200°C (normal operating conditions of a repository) is negligibly small. The same is true for the above-mentioned materials (metal sheets and tubes) up to 200°C in the two-phase system of rock salt plus NaCl-rich brine simulating the accident conditions

in a repository. In rock salt plus $MgCl_2$-rich brine, the non-corrosion protected cast steel suffers from extensive non-uniform general corrosion. However, the maximum corrosion rate of about 90 µm/a implies a technically acceptable corrosion allowance for a thick-walled container.

Slow strain rates of 10^{-4}-10^{-7} s^{-1} reduce the ductility of the steels (TStE 355, TStE 460 and 15MnNi 6.3) in the $MgCl_2$-rich brine at 90°C compared to argon which is likely due to hydrogen embrittlement. However, this effect does not appear to be serious and does not cause stress corrosion cracking for the hot-rolled steels TStE 355 and TStE 460. On the contrary, the forged steel 15MnNi 6.3 is susceptible to stress corrosion cracking in the brine at a rate of 10^{-7} s^{-1}. In view of these results, hot-rolled carbon steels and Ti 99.8-Pd continue to be considered as promising materials for long-lived HLW containers.

ACKNOWLEDGMENTS

The authors thank Prof. Dr. J.I. Kim for reviewing this paper, Mrs. R. Weiler for preparing the optical micrographs, and the Commission of the European Communities, Brussels, Belgium, for supporting this work.

6. REFERENCES

[1] E. Smailos, "Korrosionsuntersuchungen an ausgewählten Werkstoffen als Behältermaterial für die Endlagerung von hochradioaktiven Abfallprodukten in Steinsalzformationen", KfK 3953 (1985).

[2] E. Smailos, W. Schwarzkopf, R. Köster et al., "Corrosion Testing of Selected Packaging Materials for Disposal of High-Level Waste Glass in Rock Salt Formations", KfK 4723 (1990).

[3] R. Köster, "Ausgewählte Aspekte der Endlagerung radioaktiver Abfälle in Steinsalzformationen", Schriftenreihe der Universität Regensburg, Band 13, S. 71 (1986).

[4] G.H. Jenks, "Radiolysis and Hydrolysis in Salt-Mine Brines", ORNL/TM-3717, Oak Ridge National Laboratory (1972).

[5] R.G. Bates, B.R. Staples, and R.A. Robinson, "Ionic Hydration and Single Ion Activities in Unassociated Chlorides at High Ionic Strength," Analytical Chemistry 42, 8, 867 (1970).

[6] E. Smailos, B. Fiehn, J.A. Gago, I. Azkarate, "General Corrosion and Stress Corrosion Cracking Studies on Carbon Steels for Application in Nuclear Waste Disposal Containers", KfK 5166 (1993).

[7] R.E. Westerman, J.H. Haberman et al., " Corrosion and Environmental-Mechanical Characterization of Iron-Base Nuclear Waste Package Structural Barrier Materials", PNL Report No. 5426 (1986).

[8] W. Schwarzkopf, E. Smailos, R. Köster, "Langzeitbeständige Korrosionsschutzumhüllung für dicht verschlossene Gebinde mit hochradioaktivem Inhalt", DE-OS 34 47 278 (Juni 1986).

[9] W. Schwarzkopf, R. Köster, "Längszylindrischer Behälter für die Endlagerung von einer oder mehreren mit hochradioaktiven Abfällen gefüllten Kokillen", DE-OS 36 10 862 (Oktober 1987).

[10] W. Schwarzkopf, E. Smailos, R. Köster, "In-Situ Corrosion Studies on Cast Steel for a High-Level Waste Packaging in a Rock-Salt Repository", Mat. Res. Symp., Proc. Vol. 127, pp. 411-418, Materials Research Society (1988).

[11] E. Smailos, W. Schwarzkopf, J.A. Gago, I. Azkarate, "Corrosion Studies on Selected Packaging Materials for Disposal of Heat-Generating Radioactive Wastes in Rock - Salt Formations," KfK 5011 (1992).

[12] E. Smailos, W. Schwarzkopf, R. Köster, "Corrosion Behaviour of Container Materials for the Disposal of High-Level Wastes in Rock Salt Formations", Nuclear Science and Technology, CEC-Report EUR 10400 (1986).

Table I: Compositions, pH values and O_2 -contents of the salt brines used in the laboratory - scale corrosion experiments

Brine	Composition (wt.%)							
	NaCl	KCl	$MgCl_2$	$MgSO_4$	$CaCl_2$	$CaSO_4$	K_2SO_4	H_2O
1	1.4	4.7	26.8	1.4	---	---	---	65.7
2	0.31	0.11	33.03	---	2.25	0.005	---	64.3
3	25.9	---	---	0.16	---	0.21	0.23	73.5

pH (25°C): 4.6 for brine 1; 4.1 for brine 2; 6.5 for brine 3
O_2(55°C): 0.8 mg/l for brine 1; 0.6 mg/l for brine 2; 1.2mg/l for brine 3

Table II: Integral weight losses and corrosion rates of the unalloyed fine-grained steel TStE 355 after exposure to the test brines at 150°C

Brine	Test time (d)	Without gamma radiation		With gamma radiation of 10 Gy/h	
		Weight loss (g/m^2)	Corrosion rate (µm/a)	Weight loss (g/m^2)	Corrosion rate (µm/a)
1	100	178.1 ± 8.2	87.5 ± 4	367.7 ± 6.3	173.5 ± 3.0
	166	244.5 ± 15.0	68.8 ± 4.2	430.2 ± 51.7	124.0 ± 14.9
2	100	516.8 ± 20.3	254.1 ± 10.0	441.6 ± 149.4	208.4 ± 70.5
	166	605.3 ± 18.4	170.3 ± 5.2	766.0 ± 74.0	220.9 ± 21.3
3	100	50.5 ± 5.8	24.8 ± 2.9	44.9 ± 5.9	21.2 ± 2.8
	166	68.1 ± 7.1	19.2 ± 2.0	50.8 ± 6.4	14.6 ± 1.8

brines 1 and 2: $MgCl_2$-rich; brine 3: NaCl-rich

Table III: Chemical composition of the materials tested in rock salt at rock temperature (32°C) in an in-situ manner

Material	Composition (wt.%)								
	Ti	Pd	Cr	Ni	Mo	C	Si	Mn	Fe
Ti 99.8-Pd Material No. 3.7025.10	Bal.	0.18	-	-	-	0.01	-	-	0.05
Hastelloy C4 Material No. 2.4610	0.33	-	16.8	Bal.	15.9	0.006	0.05	0.09	0.05
Ni-resist D4 Material No. 0.7680	-	-	5.5	30.9	-	2.6	4.25	0.5	Bal.
Si-cast iron	-	-	-	-	-	0.72	15.0	0.62	Bal.

Table IV: Integral weight losses and corrosion rates of the materials tested in rock salt at rock temperature in an in-situ manner (test time : 9 years, T=32°C)

Material	Material condition	Weight loss (g/m^2)	Corrosion rate ($\mu m/a$)
Ti 99.8-Pd	W	- [1]	- [1]
Hastelloy C4	A	13.39±3.1	0.17±0.04
	W	28.73±24.4	0.37±0.31
Ni-resist D4	A	74.94±7.5	1.14±0.12
Si-cast iron	A	37.62±11.6	0.60±0.18

[1] no corrosion attack; A = as-received; W = TIG-welded

Table V: Mechanical properties of the parent materials investigated in the slow strain rate tests

Steel		Y.S. (0.2%) (MPa)	U.T.S. (MPa)	E (%)	R.A. (%)
TSt E 355	T	419	566	27	61
	L	427	568	28	64
TStE 460	T	505	633	24	51
	L	510	635	26	53
15MnNi 6.3	R	343	545	33	78
	Tg	340	484	29	78

T: Transversal; L: Longitudinal; R: Radial; Tg: Tangential; Y.S.: Yield strength; U.T.S. = Ultimate tensile strength; E: Elongation; R.A.: Reduction of area.

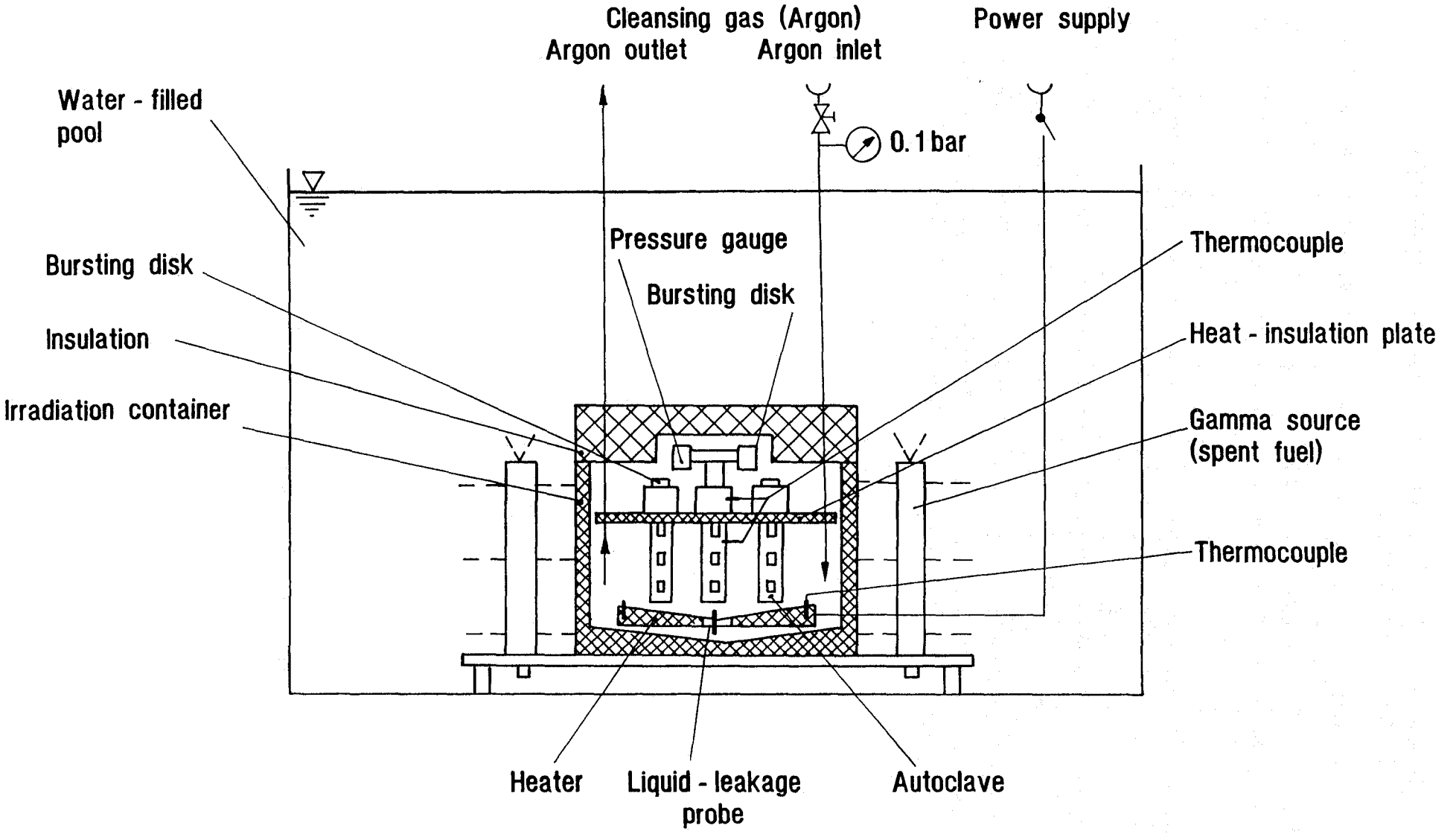

Fig. 1: Schematic of irradiation-corrosion test facility

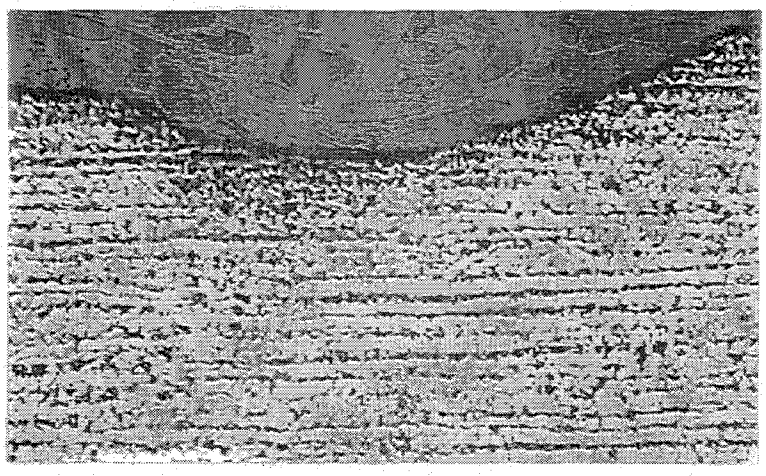

Brine 1 ($MgCl_2$-rich) X 200

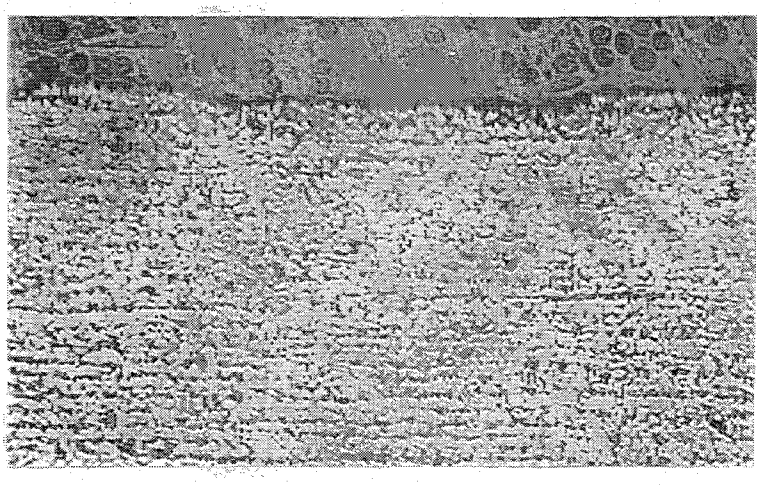

Brine 2 ($MgCl_2$-rich) X 200

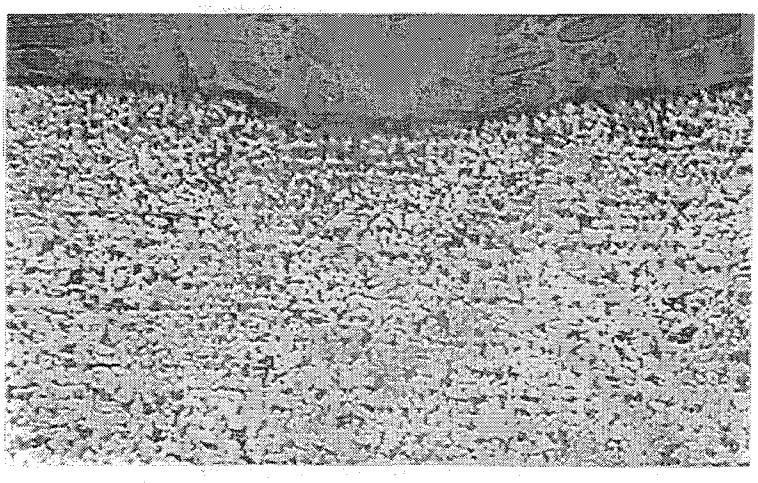

Brine 3 (NaCl-rich) X 200

Fig.2: Optical micrographs of the steel TSt E 355 after 166 days exposure to brines at 150°C and 10 Gy/h

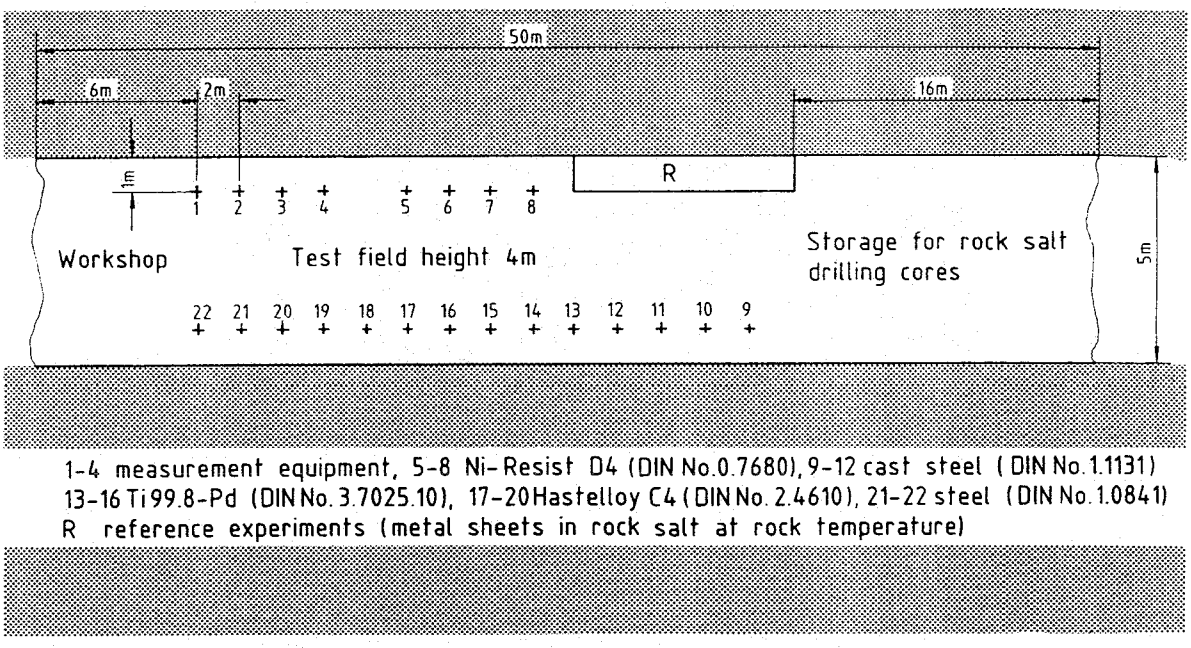

Fig. 3: Layout of the in-situ corrosion test field on the 775 m level in the Asse salt mine and arrangement of the emplacement boreholes

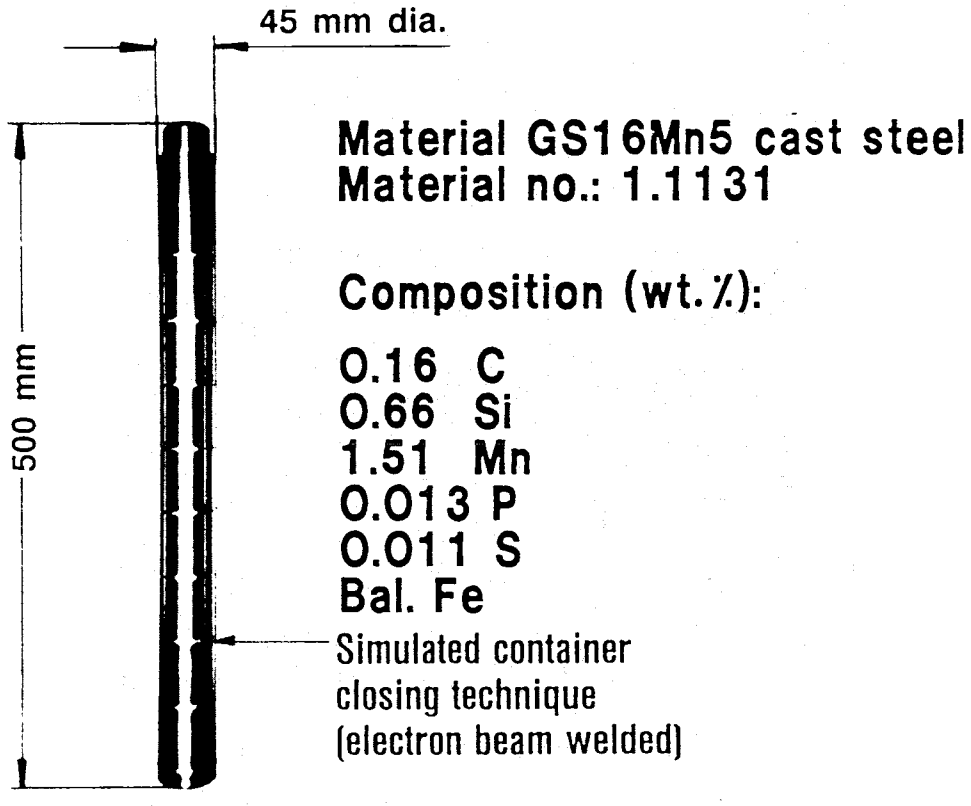

Fig. 4: Chemical composition and dimensions of cast steel specimen

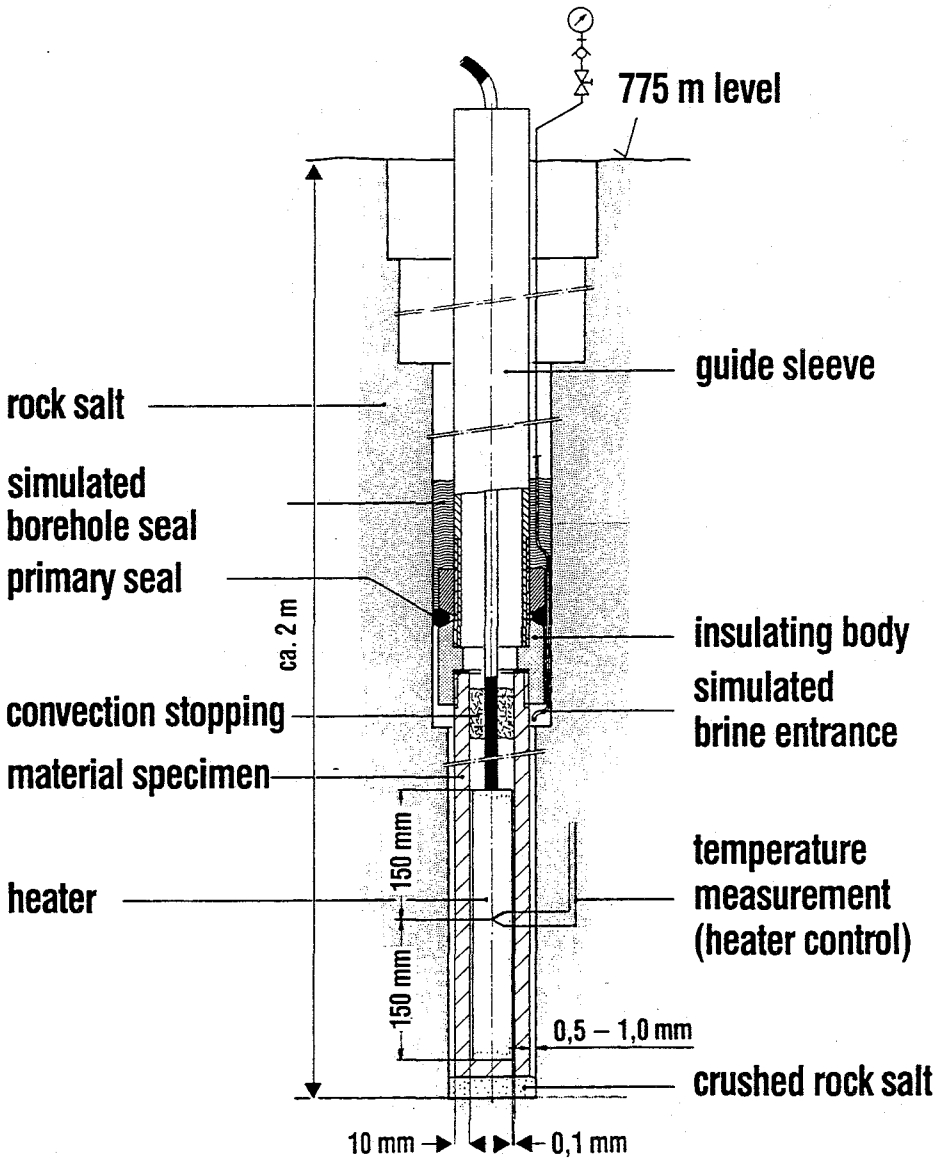

Fig. 5: Vertical cross-section of the test assembly

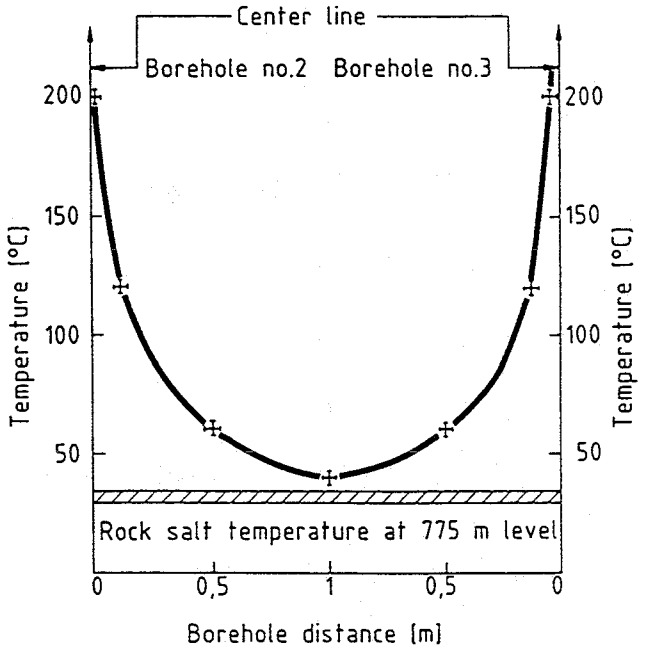

Fig. 6: Radial temperature distribution between two boreholes in the center of the heated zone

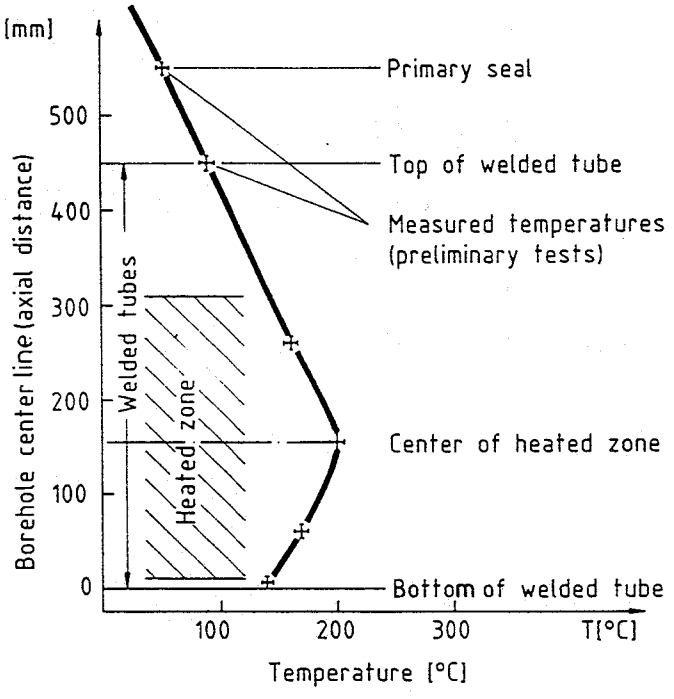

Fig. 7: Vertical temperature distribution on the welded tube wall

Fig. 8: Optical micrograph of a cast steel tube after 5.3 years in-situ testing in rock salt (0.1 wt.% H_2O) at 200°C (x 100)

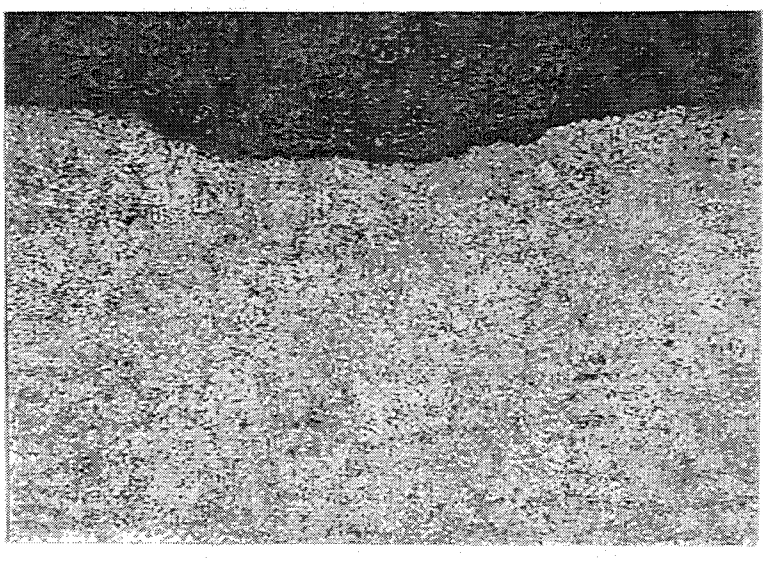

Fig. 9: Optical micrograph of a cast steel tube after 6.3 years in-situ testing in rock salt plus 100 ml $MgCl_2$-rich Q-brine at 32°C (x 32)

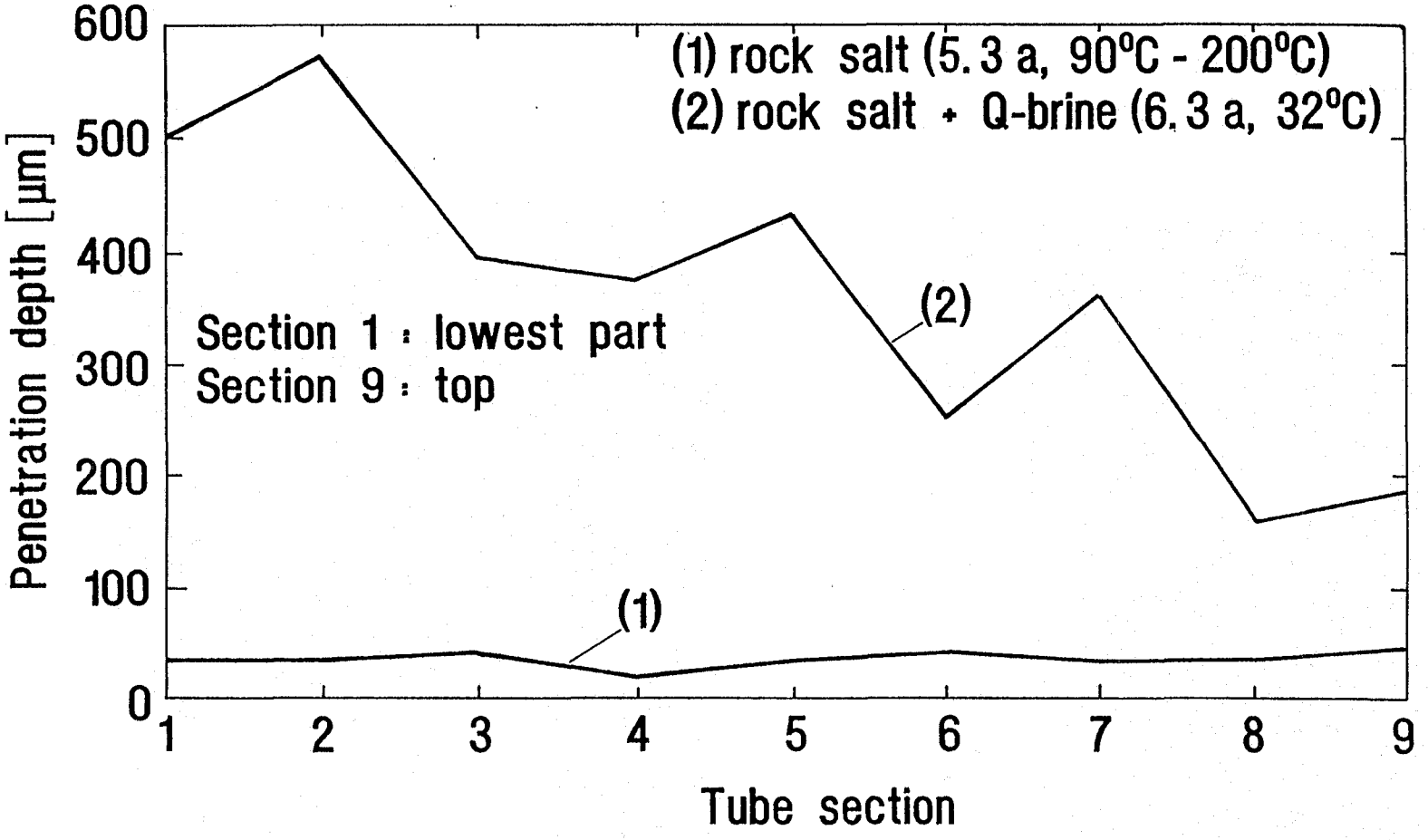

Fig. 10: Surface profilometry results of in-situ tested cast steel tubes. Maximum depth of non-uniform corrosion in rock salt and rock salt + brine

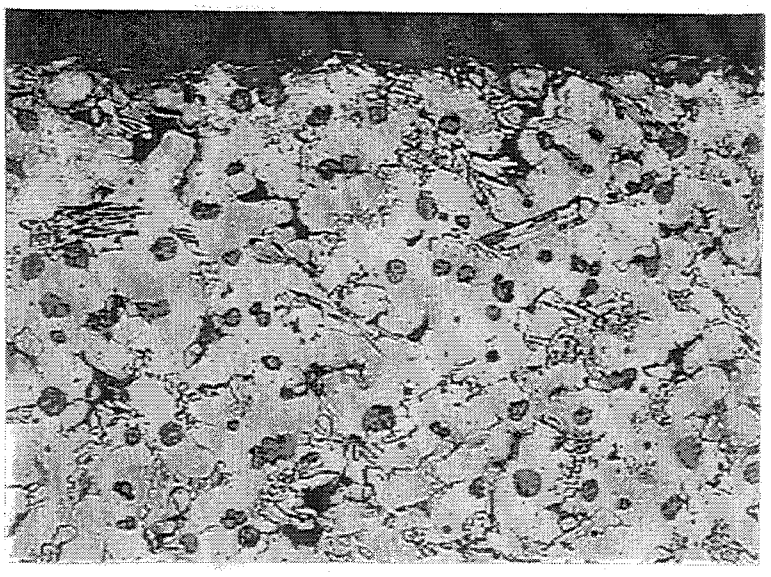

Fig. 11: Optical micrograph of a Ni-resist D4 tube after 6.3 years in-situ testing in rock salt (0.1 wt.% H_2O) at 200°C (x 100)

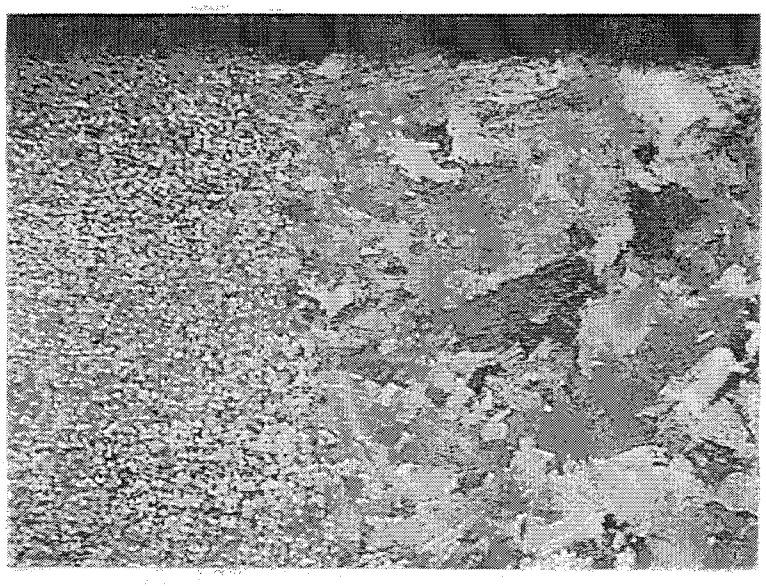

Fig. 12: Optical micrograph of a Ti 99.8-Pd tube after 2.8 years in-situ testing in rock salt plus NaCl-brine at 200°C (x 50)

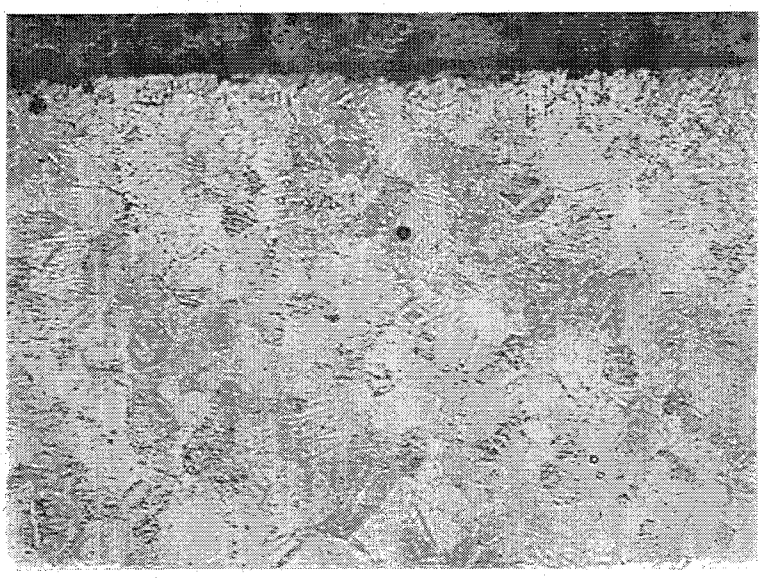

Fig. 13: Optical micrograph of the steel tube plating material Ti 99.8-Pd after 5.3 years in-situ testing in rock salt at 200°C (x 200)

Fig. 14: Optical micrograph of the steel tube plating material Hastelloy C4 after 6.3 years in-situ testing in rock salt plus NaCl-brine at 32°C (x 200)

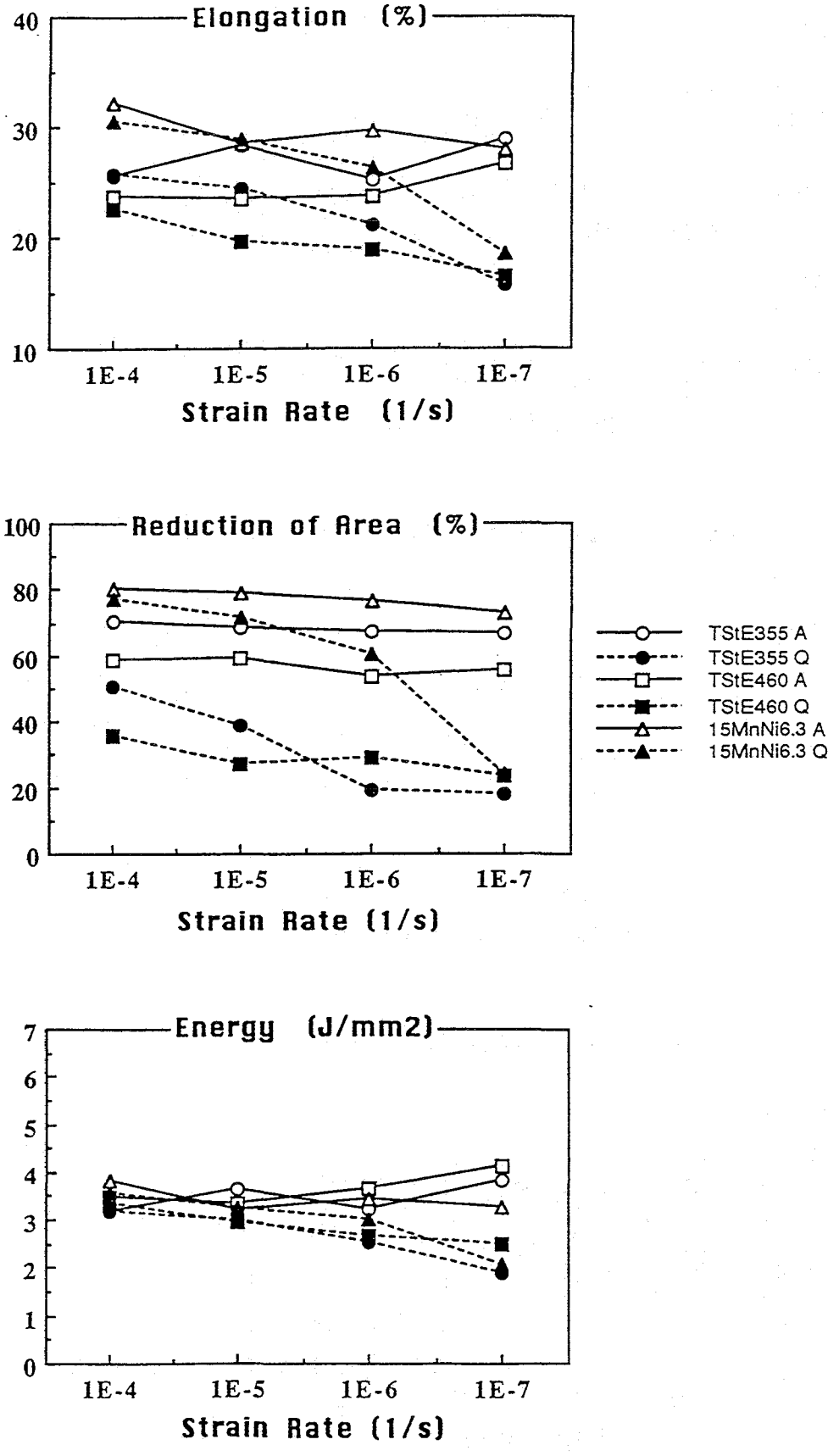

Fig. 15: Elongation, reduction of area and energy versus strain rate for the steels TStE 355, TStE 460 and 15MnNi6.3 tested at 90°C and 13 MPa in argon and Q-brine

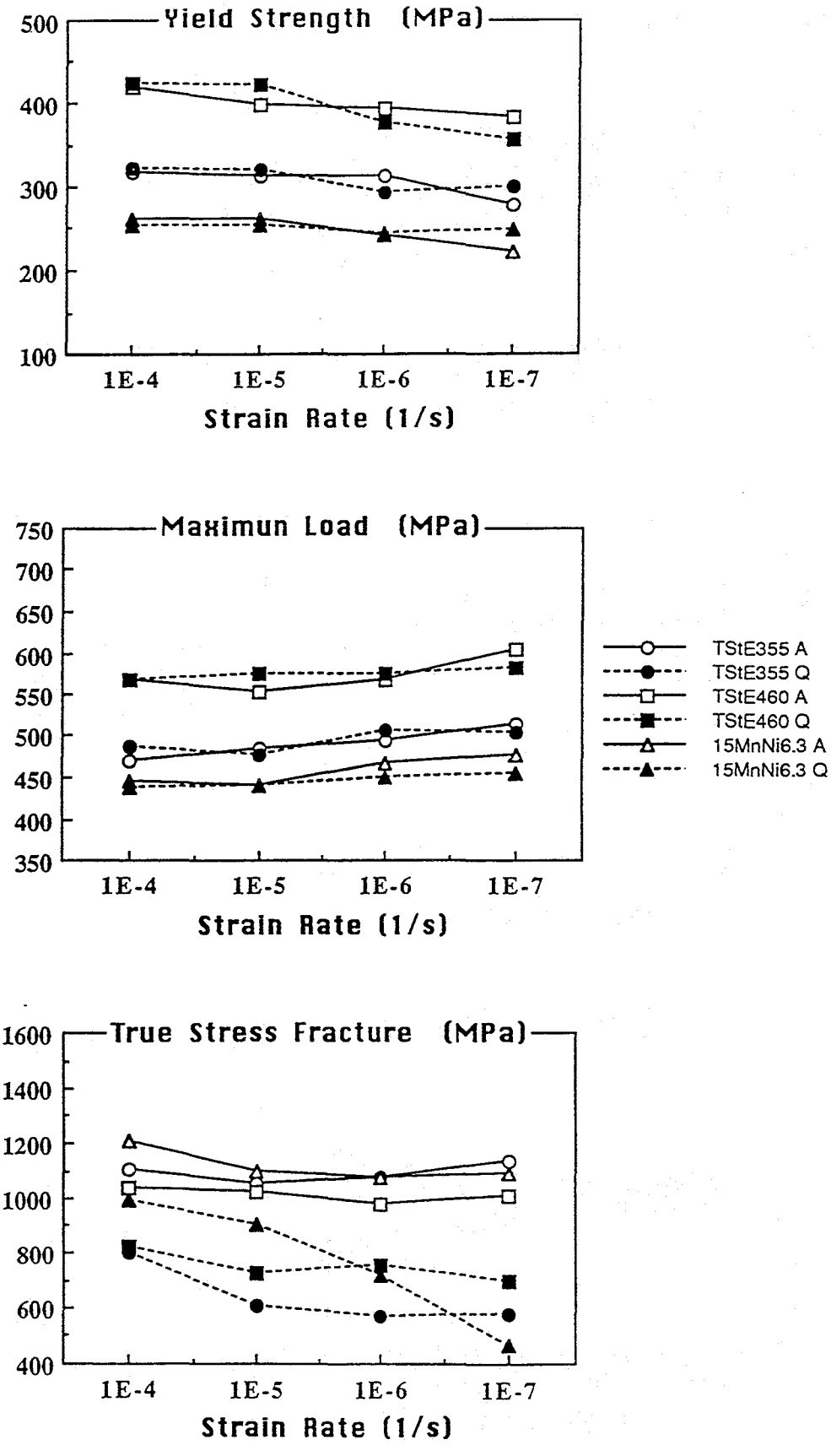

Fig. 16: Yield strength, maximum load and true stress fracture versus strain rate for the steels TStE 355, TStE 460 and 15 MnNI6.3 tested at 90°C and 13 MPa in argon and Q-brine

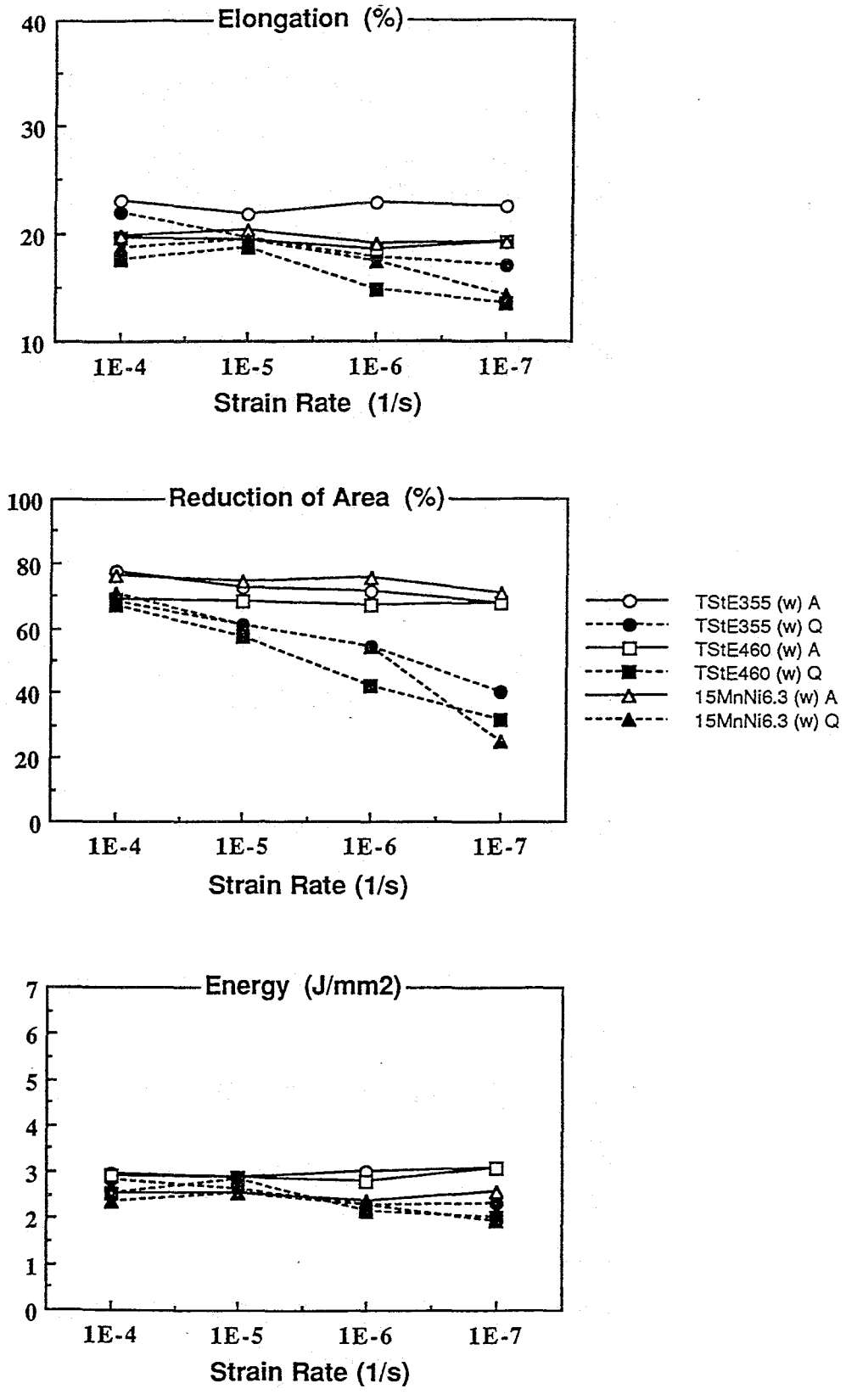

Fig.17: Elongation, reduction of area and energy versus strain rate for the MAG welded steels TStE 355, TStE 460 and 15 MnNi 6.3 tested at 90°C in argon and Q-brine

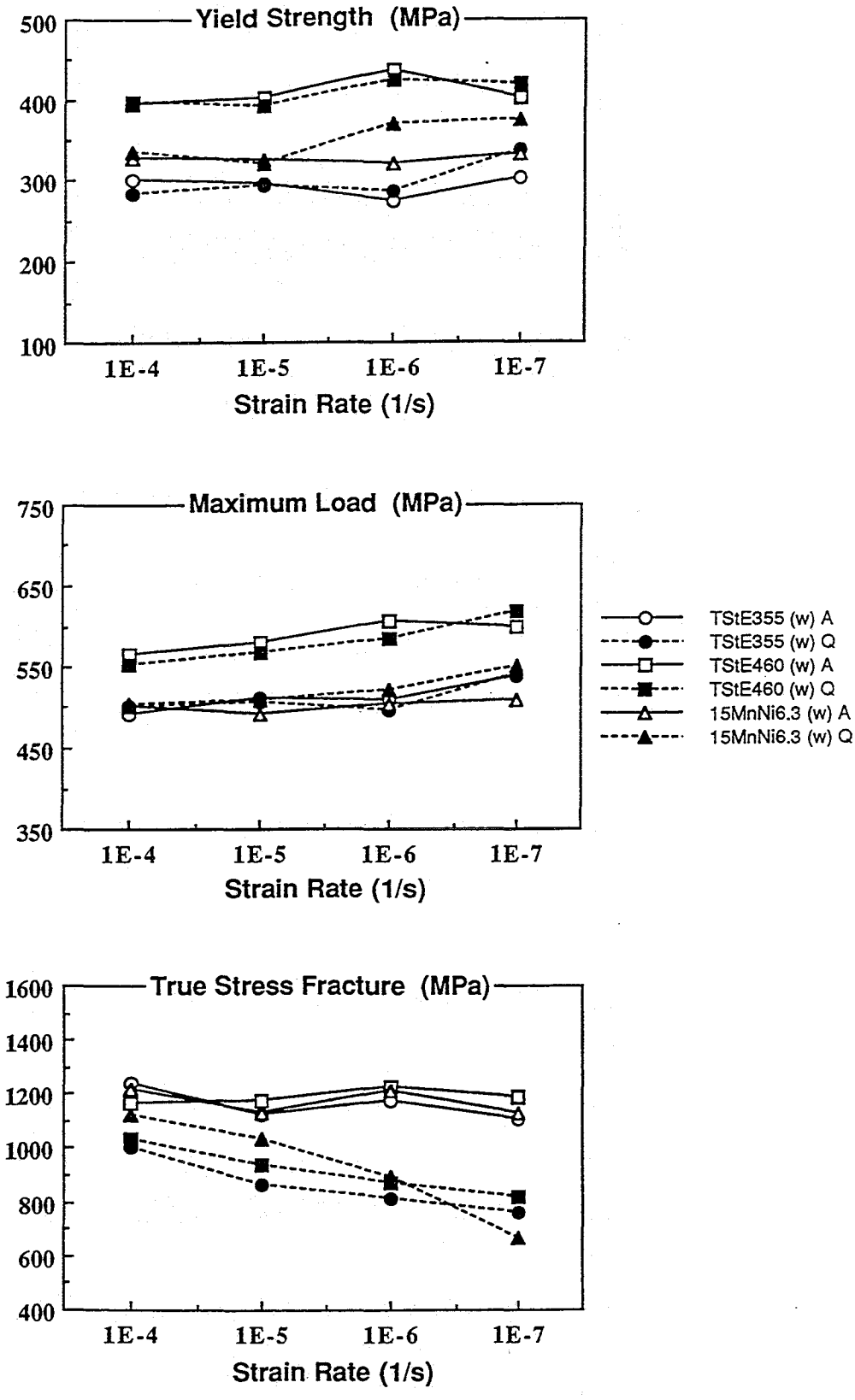

Fig.18: Yield strength, maximum load and true stress fracture versus strain rate for the MAG welded steels TStE 355, TStE 460 and 15 MnNi 6.3 tested at 90°C in argon and Q-brine

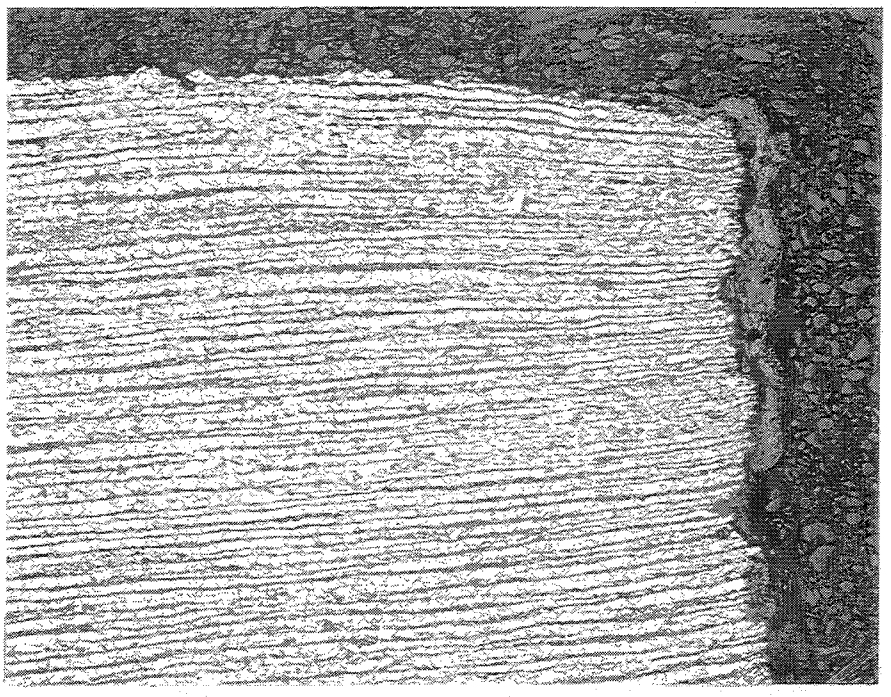

Fig. 19: Optical micrograph of a tensile specimen of the steel TStE 355 tested in Q-brine at 90°C, 13 MPa and a strain rate of $10^{-7}s^{-1}$ (x 100)

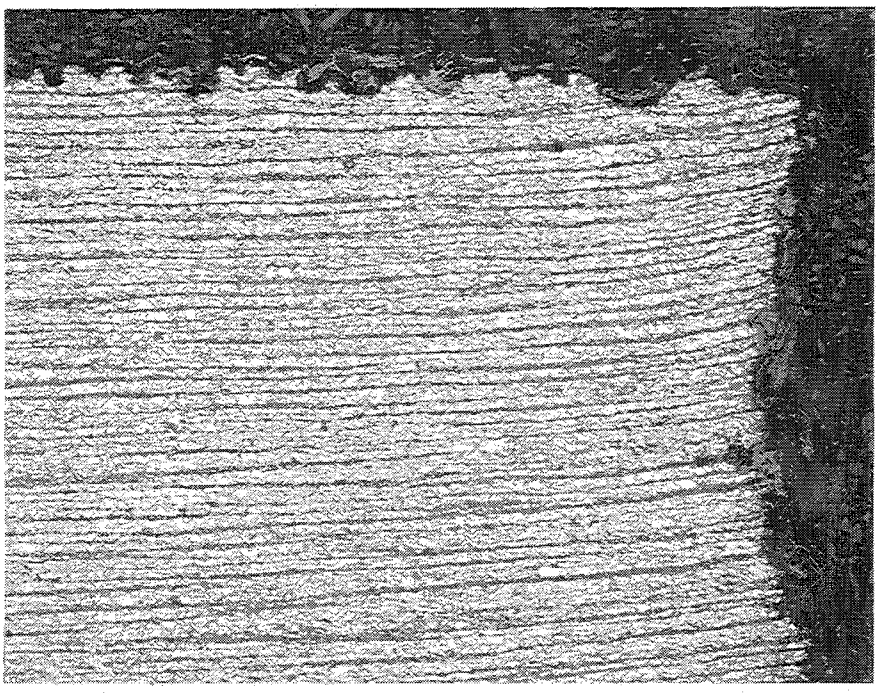

Fig. 20: Optical micrograph of a tensile specimen of the steel TStE 460 tested in Q-brine at 90°C, 13 MPa and a strain rate of $10^{-6}s^{-1}$ (x 100)

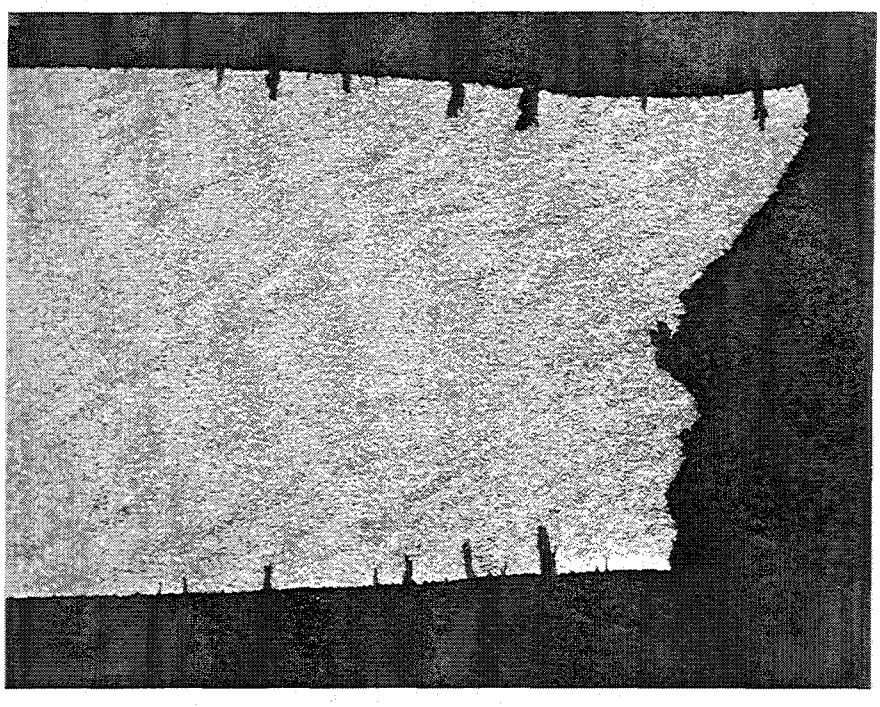

Fig. 21: Optical micrograph of a tensile specimen of the steel 15MnNi 6.3 tested in Q-brine at 90°C, 13 MPa and a strain rate of $10^{-7}s^{-1}$ (x 12)

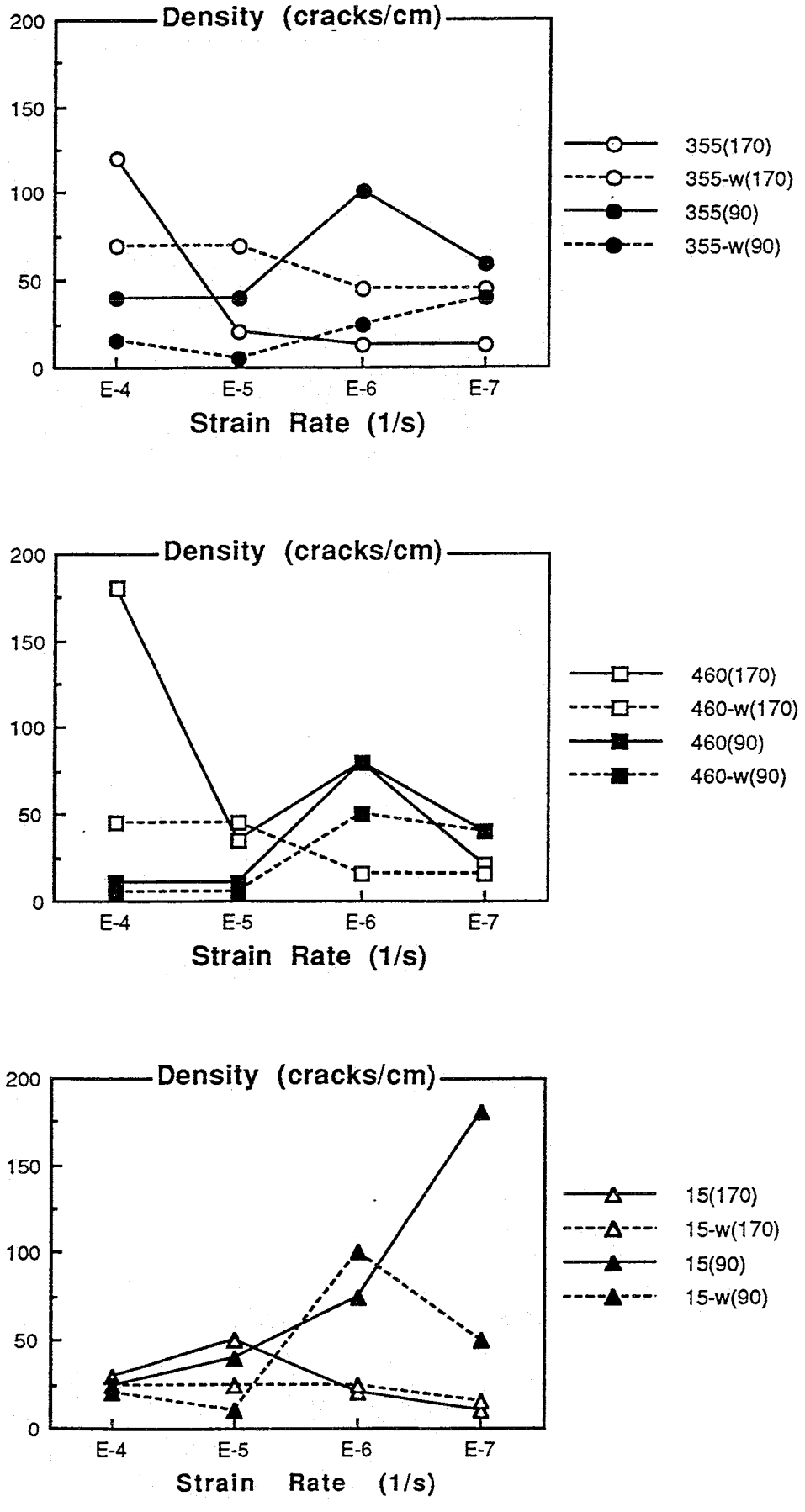

Fig. 22: Crack density obtained for the steels TStE 355, TStE 460 and 15MnNi 6.3 after slow strain rate testing in Q-brine under various conditions (T = 90°C, 170°C, w = welded material)

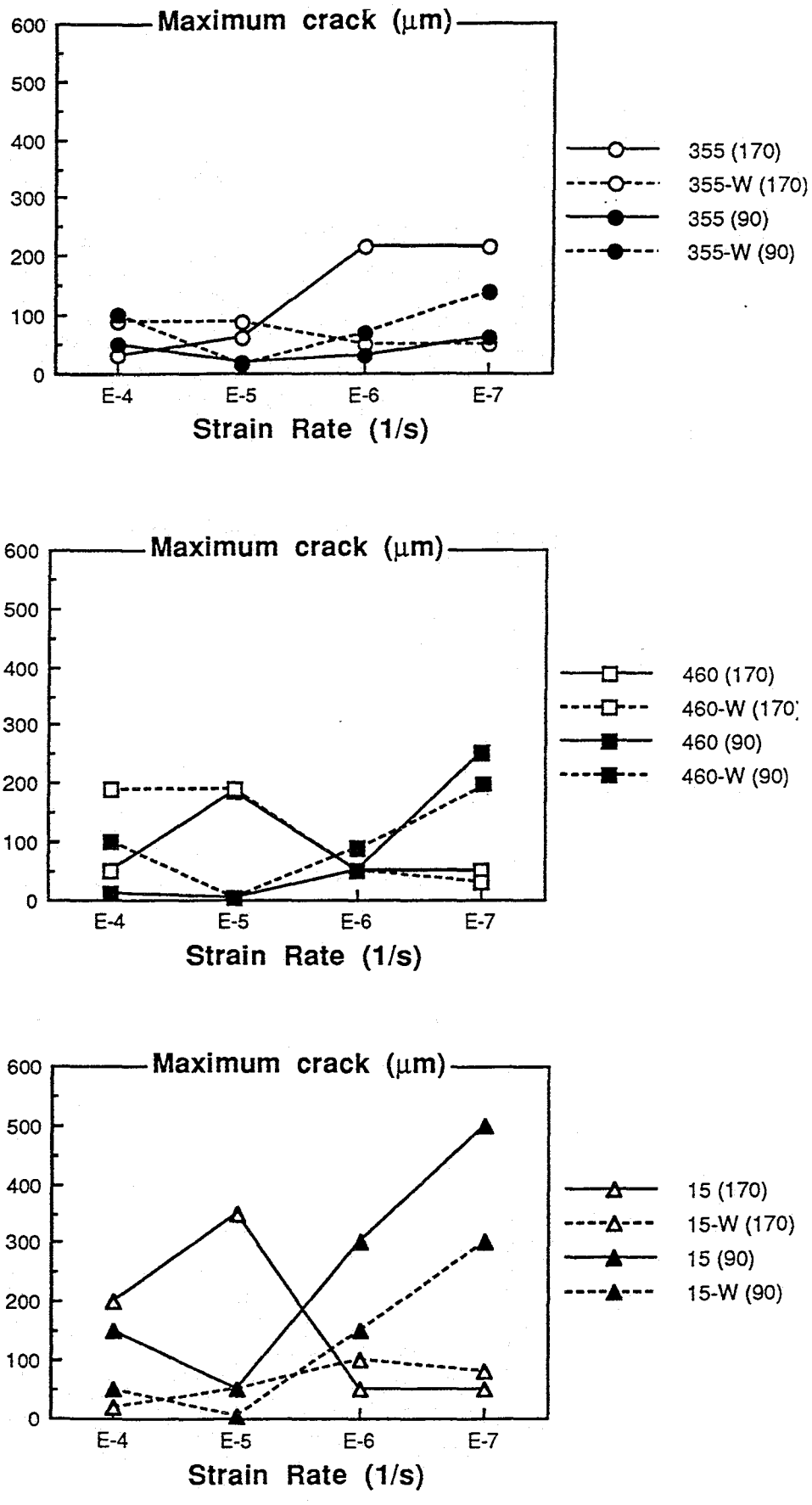

Fig. 23: Maximum crack length obtained for the steels TStE 355, TStE 460 and 15MnNi 6.3 after slow strain rate testing in Q-brine under various conditions (T = 90°C, 170°C, w = welded material)

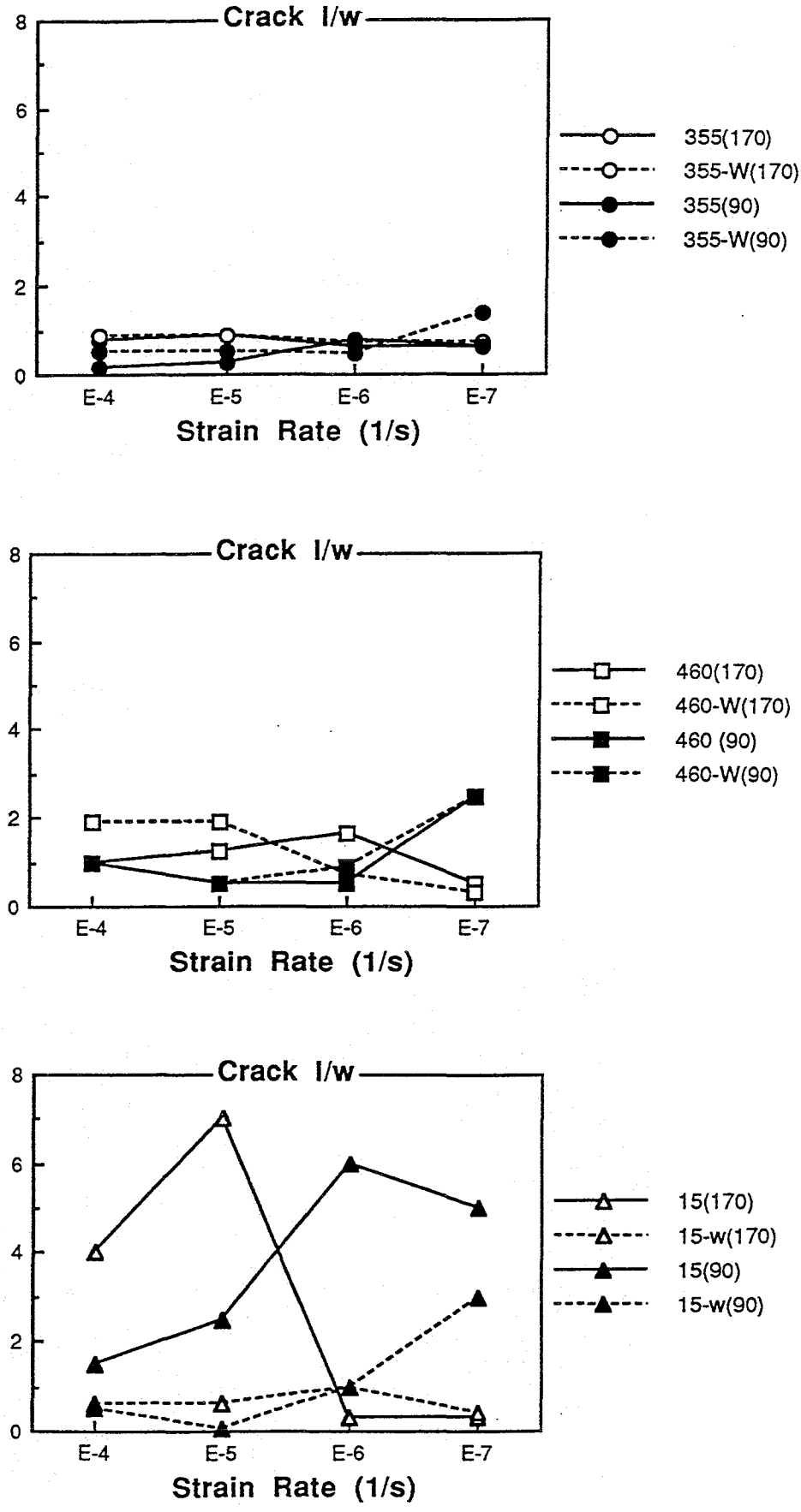

Fig. 24: Crack length to wide ratio obtained for the steels TStE 355, TStE 460 and 15MnNi 6.3 after slow strain rate testing in Q-brine under various conditions (T = 90°C, 170°C, w = welded material)

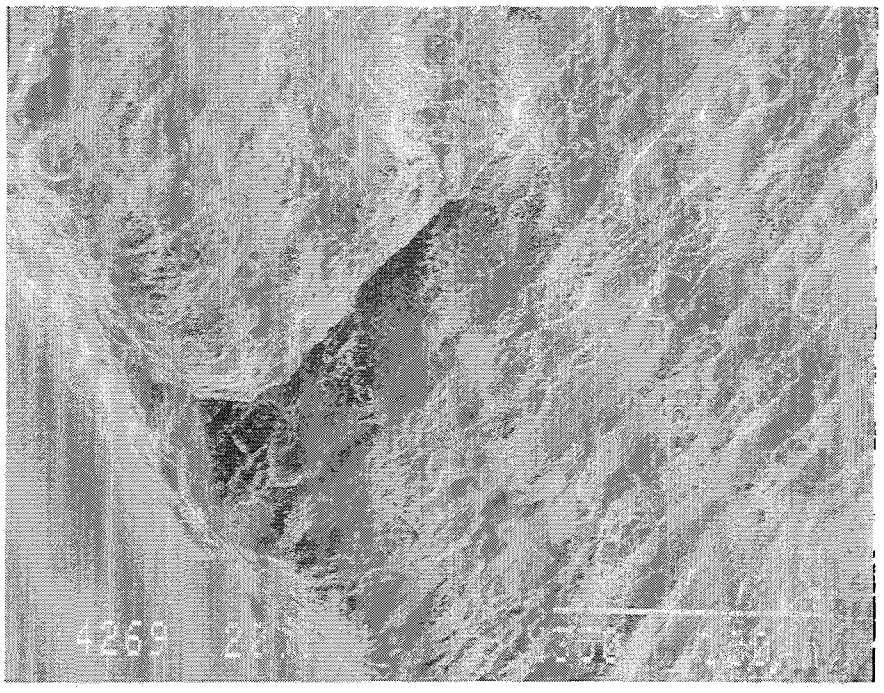

Fig. 25: Fracture surface of a TStE 355 steel specimen tested in Q-brine at 90°C, 13 MPa and $10^{-6}s^{-1}$ (x 350)

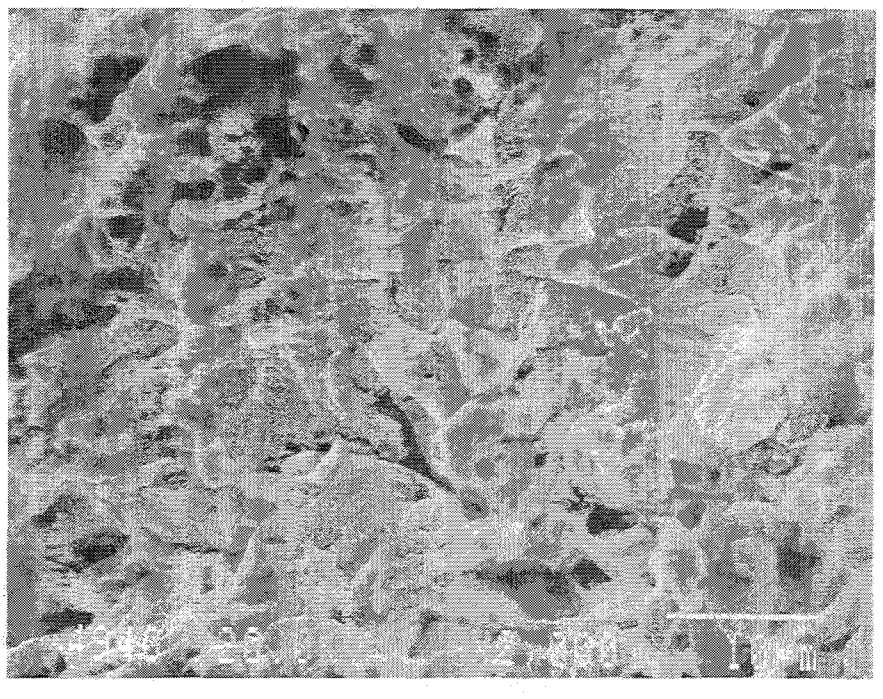

Fig. 26: Fracture surface of a TStE 460 steel specimen tested in Q-brine at 90°C, 13 MPa and $10^{-6}s^{-1}$ (x 2000)

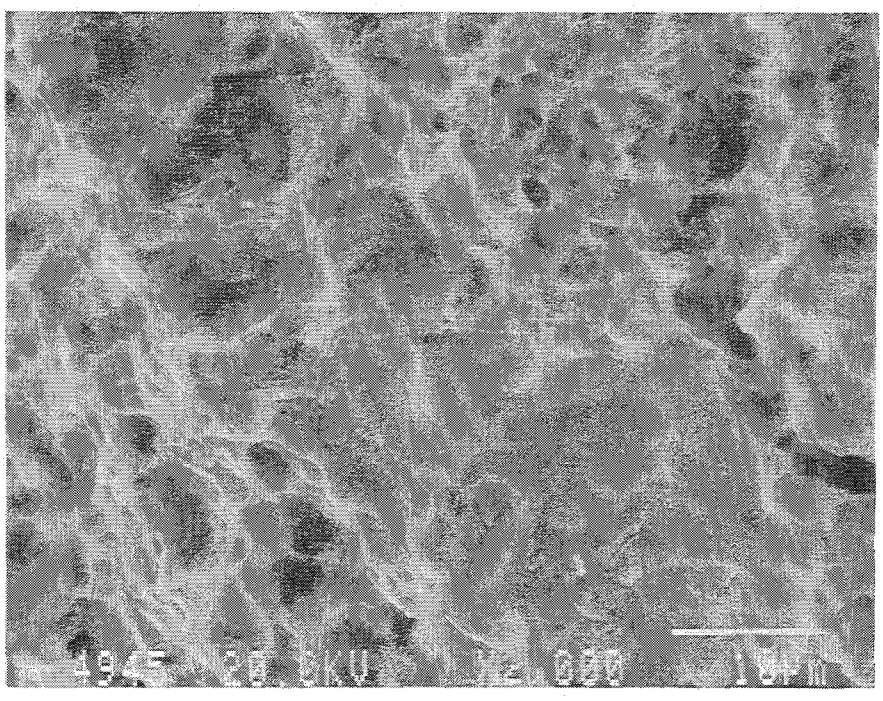

Fig. 27: Fracture surface of a 15MnNi 6.3 steel specimen tested in Q-brine at 90°C, 13 MPa, and $10^{-7}s^{-1}$ (x 2000)